Marine Mammal Science

ARTICLE OPEN ACCESS

Seasonal and Interannual Variation of Common Dolphin, *Delphinus delphis*, Density in Portuguese Waters

Miguel P. Martins[1,2,3] | Marc Fernandez[4,5] | Ana Marçalo[6] | Nuno Oliveira[7] | Tiago A. Marques[1,2,8]

[1]Faculdade de Ciências, Universidade de Lisboa, Lisbon, Portugal | [2]CREEM – Centre for Research Into Ecological and Environmental Modelling, the Observatory, University of St Andrews, St Andrews, UK | [3]AIMM – Associação Para a Investigação Do Meio Marinho, Lisbon, Portugal | [4]MARE – Marine and Environmental Sciences Centre, ARNET – Aquatic Research Network, Regional Agency for the Development of Research, Technology and Innovation (ARDITI), Funchal, Portugal | [5]University of Madeira, Funchal, Portugal | [6]Centre of Marine Sciences (CCMAR), CIMAR LA – Centro de Investigação Marinha e Ambiental Laboratório Associado, Campus de Gambelas, University of the Algarve, Faro, Portugal | [7]SPEA – Sociedade Portuguesa Para o Estudo das Aves, Marine Conservation Department, Lisboa, Portugal | [8]DBA - Departamento de Biologia Animal, Faculdade de Ciências da Universidade de Lisboa, Lisbon, Portugal

Correspondence: Miguel P. Martins (mpmartins@ciencias.ulisboa.pt)

Received: 25 June 2025 | **Revised:** 23 February 2026 | **Accepted:** 5 March 2026

Keywords: common dolphin | density surface models | distribution | population size

ABSTRACT

Modeling a species' ecology and abundance provides important insights into its habitat preferences, population trends, and distribution. Here, we studied how environmental factors relate to common dolphin (*Delphinus delphis*) density in waters off mainland Portugal. We analyzed an opportunistic dataset collected using European Seabirds at Sea (ESAS) methodology within a distance sampling framework, spanning from 2004 to 2020. We fitted habitat-based Density Surface Models (DSMs) relating common dolphin counts, corrected for detectability, to environmental factors. We found significant effects of distance to the coast—varying seasonally—and a selection of dynamic covariates on dolphin density. We then predicted and mapped common dolphin density throughout the sampling period. Predictions were restricted to coastal regions in spring and winter, due to a lack of offshore effort. Coastal abundance was highest during the summer. When accounting for the entire EEZ, estimated abundance was greatest during autumn, although with considerably large uncertainty measures. Distribution along the coast was patchy across all seasons. Offshore densities were higher in the autumn than in the summer. These results highlight the spatiotemporal distribution and abundance fluctuations of common dolphins, demonstrating how, when treated carefully, opportunistic data can fill in the blanks on species ecology and abundance.

1 | Introduction

Estimating species distributions, abundance, and associated trends are fundamental for population conservation and management. Despite this, there are still great gaps in our knowledge of cetacean densities, with large areas of the oceans still not surveyed or with insufficient effort to allow for trend analysis (Kaschner et al. 2012). Distance sampling is a widely used methodology to achieve unbiased abundance and density estimates. By recording the distance an object is from a trackline, one can fit a model of the detection probability conditional to the distance, that is, a detection function, allowing to correct the number of animals sighted for their detectability (Buckland et al. 2001). The detection function can be further improved by accounting for covariates besides distance that also impact detectability (Marques et al. 2007). Line transect sampling is the primary approach used for estimating cetacean abundance (Hammond, Francis, et al. 2021). Conventional methods are usually design based, but transects can be split into segments, and counts per segment, corrected for detectability, can then be modeled to produce model-based abundance estimates conditional to environmental variables (Miller et al. 2013). The model results can then be projected in space, creating spatially explicit density estimates that reflect the animal's distribution (Miller et al. 2013; Roberts et al. 2016). These models are referred to as Density Surface Models (DSMs). DSMs can be fitted in either a one- or two stage-approaches. In the former the parameters of the detection function and the spatial/environmental model are estimated at the same time, while in the latter the detection function and the spatial/environmental model are fitted separately (Miller et al. 2013).

As of 2012, about 25% of the global ocean surface had been covered by line transect surveys dedicated to studying cetacean abundance (Kaschner et al. 2012). Since then, sampling effort has increased worldwide (e.g., Bedriñana-Romano et al. 2022; Carretta et al. 2024), however, there are still large areas of the ocean that have not been properly surveyed. Systematic efforts like the North Atlantic Sighting Survey (NASS) and the Small Cetaceans in European Atlantic waters and the North Sea (SCANS) surveys have brought insight into the summer abundance and distribution of cetacean species in the eastern and central north Atlantic (Gilles et al. 2023; Pike et al. 2019) but remain rare. Despite large, dedicated surveys not occurring yearly, and uneven spatial coverage throughout the years, sampling effort in European Atlantic waters has been extensive enough to allow for some trend analysis. Yet, there has been notably less effort in the western and southern waters of continental Europe. In mainland Portugal, sampling effort has been restricted to coastal areas until only the last SCANS-IV survey, where it was expanded offshore (Gilles et al. 2023; Hammond, Lacey, et al. 2021; Vingada and Eira 2018). Additionally, sampling effort is typically restricted to, or heavily concentrated in, the summer months. Therefore, we have an incomplete understanding of the seasonal and interannual variation of cetaceans' abundance and distribution in the region, especially in offshore waters. Portuguese waters are included in the Canary/Iberian Eastern Boundary Upwelling System (Bakun et al. 2015), among the most productive marine ecosystems in the world. This makes the area suitable for the occurrence of marine megafauna (Couto et al. 2017, 2018; Martins et al. 2025). This region is of particular interest to study cetaceans, having 30 confirmed species recorded, through sightings and strandings (Mathias et al. 2024; Morais et al. 2021; Moura et al. 2017; Sabino-Marques 2005; Vingada and Eira 2018).

Despite lower survey effort, when compared with other European waters, it is clear that the common dolphin (*Delphinus delphis*) is the most abundant cetacean in Portugal, with the most recent abundance estimate at 76,615 individuals over an area of 210,991 km^2 (Gilles et al. 2023). This corresponds to an average density of 0.36 individuals/km^2 in Portuguese waters. However, this estimate is for only about 68% of the total Portuguese Exclusive Economic Zone (EEZ)—here defined as the sum of the area of the EEZ itself, territorial sea and inland maritime waters (DGRM 2018). This globally distributed species has a patchy distribution along Portuguese coastal waters, its occurrence being largely related to high primary production (Moura et al. 2012). In fact, its occurrence has been associated with upwelling modified habitats (Au and Perryman 1985), which create suitable conditions for the small pelagic fishes the dolphin targets, like the sardine (*Sardina pilchardus*)–the most important prey item on the common dolphin's diet in mainland Portugal (Marçalo et al. 2018). The common dolphin tends to prefer coastal areas, although its presence is also detected at lower density in offshore environments (Gilles et al. 2023). Despite occurring in both tropical and temperate waters, the common dolphin's habitat suitability has been related to relatively low ($<20°C$) sea surface temperature (SST) in the Eastern North Atlantic (Fernandez et al. 2021). With climate change, it is expected that the ranges of the common dolphin and its preferred prey will expand towards higher latitudes (Lima et al. 2022; MacLeod 2009; Sousa et al. 2023).

In this study, we model 16 years of common dolphin densities, through habitat-based DSMs, from an opportunistic line transect dataset that spans over the entire Portuguese EEZ. We also discuss potential climate change and overfishing impacts on the common dolphin's density.

2 | Methods

2.1 | Data Collection

Cetacean occurrence data and corresponding sampling effort were provided by the Portuguese Society for the Study of Birds. Data collection occurred between December 2004 and December 2020 by experienced observers onboard several types of vessels (e.g., research vessels of the Portuguese Institute for Sea and Atmosphere—IPMA—used opportunistically, direct surveys using small-medium size motor vessels or sailing boats, etc.) using the European Seabird at Sea Methodology (ESAS) (Tasker et al. 1984). IPMA survey vessel lengths were 46–70 m where the observation platform was located at 5–15 m above sea level. Small/medium vessels were 12–15 m long with the observer platform ranging from 2 to 5 m above sea level. IPMA surveys were designed to run annual stock assessments of small pelagic fishes in Portuguese waters. Location, time of year, length, and design of those surveys were then selected to fulfill that goal. Those surveys were opportunistically used to collect data on megafauna, including cetaceans, seabirds, and marine turtles. Surveys took place roughly every year (during Spring and Autumn) along the time series. In addition, several campaigns were run in specific years and periods of the year to fill the temporal and spatial gaps derived from the IPMA surveys. Those campaigns allowed a better balance on temporal and spatial coverage and were designed to primarily collect data on megafauna.

The vessels followed a line transect protocol. All observers were previously trained in cetacean identification and on the ESAS methodology. Observers were placed mostly at the bow of the vessel searching forward (i.e., in the direction of the vessel movement) and on one side of the vessel. The set-up for data collection is a 90 degrees angle of view to be selected from bow to beam, based on the side of the vessel that affords the best combined viewing conditions. Observers calibrate their distance estimates several times during the daily surveying period using a range stick, made specifically for each observer and observation platform. The 300 m limit was assessed in the field using a range finder. Observers empirically assigned the radial distance estimate to an appropriate distance band in the field. Distance to the line was recorded in intervals, during data collection, into five categories: (i) 0–50 m; (ii) 50–100 m; (iii) 100–200 m; (iv) 200–300 m and (v) > 300 m. Cetaceans were recorded on one side of the boat and sightings were included for analysis only when the perpendicular distance to the transect line was less than 300 m. All detected mammals were identified to the smallest possible taxonomic unit, counted, and their behavior recorded.

The sampled area was surveyed by a team of two, with one surveyor observing and verbally relaying data to a second who recorded the information onto survey forms or on a tablet (Samsung Galaxy Tab A 8.0, 8″, 2 GB ROM) with an electronic App (CyberTracker), in addition to providing supplementary observations. In circumstances where it was only possible to use one observer, the observer was sufficiently experienced and aware of the need to take regular breaks so that data quality was not compromised by fatigue. For surveys comprising more than 8 h of continuous observation effort per day, a second team of two observers were used to allow rotation of observation teams to prevent fatigue. Handheld GPS units or the electronic App were used to record tracks while surveys have been carried out. Survey effort was suspended when sea conditions were too rough, that is, winds stronger than Beaufort scale 5 (> 39 km/h).

2.2 | Environmental Variables

A set of 10 environmental variables was used for modeling and predicting common dolphin density (Table 1). Five static variables were considered (seafloor depth, seafloor slope and distances to the coast, to the 200 m and 1000 m isobathymetric lines). These variables were derived from an esriAscii file containing a digital terrain model (DTM) for bathymetry (seafloor depth at a given location), downloaded from the GEBCO initiative on 30/09/2024 (GEBCO 2025). Depth was read directly from the DTM in R, version 4.4.1 (R Core Team 2024) using the raster package (Hijmans 2023). From the DTM file, the seafloor slope was calculated in R using the terrain function from the raster

TABLE 1 | Variables considered for modeling and predicting common dolphin density.

Variable	Acronym/ Abbreviation	Temporal resolution	Spatial resolution	Units	Source/Product ID
Seafloor depth	Depth	NA	0.083°	m	GEBCO
Seafloor slope	Slope	NA	0.083°	°	GEBCO
Distance to the coast	DTC	NA	0.083°	m	GEBCO
Distance to the 200 m isobathymetric line	DT200	NA	0.083°	m	GEBCO
Distance to the 1000 m isobathymetric line	DT1000	NA	0.083°	m	GEBCO
Sea surface temperature	SST	8D	0.083°	°C	Atlantic-Iberian Biscay Irish-Ocean Physics Reanalysis. Product identifier: IBI_ MULTIYEAR_PHY_005_002
Chlorophyll-a concentration	CHL	8D	0.083°	mg/m^3	Atlantic-Iberian Biscay Irish-Ocean BioGeoChemistry NON ASSIMILATIVE Hindcast. Product identifier: IBI_ MULTIYEAR_BGC_005_003
Chlorophyll-a concentration with 3-month lag	CHL-lag3	8D	0.083°	mg/m^3	Atlantic-Iberian Biscay Irish-Ocean BioGeoChemistry NON ASSIMILATIVE Hindcast. Product identifier: IBI_ MULTIYEAR_BGC_005_003
Salinity	Salinity	8D	0.083°	10^{-3}	Atlantic-Iberian Biscay Irish-Ocean Physics Reanalysis. Product identifier: IBI_ MULTIYEAR_PHY_005_002
Mass content of zooplankton expressed as carbon in sea water	Zooplankton	8D	0.083°	g/m^2	Global ocean low and mid trophic levels biomass content hindcast. Product identifier: GLOBAL_ MULTIYEAR_BGC_001_033

Abbreviations: 8D, 8-day composite; NA, non-applicable; Y, yearly.

package (Hijmans 2023). Distance to the coast and to the 200 and 1000 m isobathymetric lines were derived from the DTM using the dist2isobath function from the marmap R package (Pante et al. 2023). Static environmental variables were downloaded with a spatial resolution of 15 arcsec.

We used five dynamic variables: chlorophyll-a concentration (with and without a 3-month time lag), sea surface temperature (SST), salinity, and surface zooplankton concentration as proxies for prey distribution in Portuguese waters. These variables have been shown to affect sardine—the primary prey of common dolphins in this region (Marçalo et al. 2018)—distribution and growth along the Portuguese coast and adjacent waters. The spatial chlorophyll-a and phytoplankton concentrations represent sardine food availability as this fish feeds primarily on phytoplankton and, to a lesser extent, zooplankton (Garrido et al. 2008). Three-month time lags of chlorophyll-a concentration peaks have also been correlated with maximum sardine body condition and growth (Rueda et al. 2015; Silva et al. 2008). Finally, sardines tend to prefer waters with temperatures below 20°C and high salinity (Lima et al. 2022).

These dynamic variables were obtained from the Copernicus Marine system at daily temporal resolution and 0.083° spatial resolution. Eight-day composites were then created using the calc function from the raster R package. The composites were extracted to both segment centroids (the approximate center of each transect segment) and prediction grid points (a dataset reflecting the environmental conditions of the study area for model prediction) based on their location and date using the raster package.

To maintain consistent spatial resolution across environmental variables, we resampled the static variables to match the coarser resolution of the dynamic variables using the resample function from the terra R package (Hijmans 2025).

2.3 | Data Preparation

Transect segments were created, each corresponding to 5 min of sampling, resulting in 48,875 segments (mean length: 1.28 km, SD = 0.31 km). Two datasets were created for analysis. The first contained common dolphin observations, including group size, perpendicular distance to the transect line, and geographic location. The second contained segment-level data, including distance traveled, geographic location, and environmental conditions at the segment centroid. Observations were linked to their corresponding segments for modeling.

Geo-referenced prediction grids, with a 1 km^2 resolution, approximating the grid's spatial resolution to the average segment's resolution, representing the Portuguese EEZ, were created using QGIS (QGIS Development Team 2024). The shapefile used to create the grid was downloaded from ArcGIS Hub (2024). Spatially explicit environmental conditions were attributed to the segment dataset and prediction grids using the extract function from the raster package. Each prediction grid reflected the environmental conditions of the week at the midpoint of each season (winter, spring, summer, and autumn) throughout the sampling period (2004–2020). The considered midpoints were the 2nd of February, the 6th of May, the 6th of August, and the 6th of October, for winter, spring, summer, and autumn, respectively.

Additional prediction grids were created to facilitate comparisons with existing literature. Two new sets were constructed: (1) one for the SCANS-IV survey blocks where common dolphins were detected in mainland Portugal (ICC, ICE, ICF, and ICG) and (2) another for the overlapping area between this study's study region and SCANS-III blocks AA and AB. Shapefiles for SCANS-III survey blocks were retrieved from/and for SCANS-IV shapefiles from https://www.tiho-hannover.de/en/clinics-institutes/institutes/institute-of-terrestrial-and-aquatic-wildlife-research-itaw/scans-iv-survey.

Environmental conditions were extracted for each grid to match the temporality of each survey. For the SCANS-III blocks' grids, we extracted the environmental conditions for summer 2016, when the survey was conducted (Hammond, Lacey, et al. 2021). For the SCANS-IV blocks' grids, we extracted the environmental conditions for summer 2020, the closest period in our data to the time when the survey was conducted (Gilles et al. 2023).

2.4 | Two-Stage Density Surface Modeling

A two-stage density surface modeling approach was used, starting with fitting detection functions to allow for the correction of observed counts for detectability, followed by fitting an environmentally explicit density model to the corrected counts, following Miller et al. (2013).

2.4.1 | Detection Function

Detection functions were fitted to model common dolphin's detection probability conditional to the distance to the transect line, using the ds function from the Distance R package (Miller et al. 2019). Three key-functions (uniform, half-normal, and hazard-rate) were tested. For the uniform key, detection functions with 0, 1, and 2 cosine adjustments were tested. For the half-normal and hazard-rate keys, cosine adjustments were not used, but sea state, in the Beaufort scale, was incorporated as a covariate. We tested models without covariates, as well as models where sea state was either a continuous or a factor variable. Since there were few records with sea state ≥ 4, all of these were aggregated in a single level for the factor sea state covariate. The plausibility of the shape of the detection function was fundamental to choose between different models considered for the detection function.

2.4.2 | Spatial Model Fitting

Before modeling, Pearson's correlation coefficient between all pairs of environmental variables was calculated. If the correlation was > 0.7 (see Figure S1), the correlated variables were not included in the same model and were tested in different models (see Table S1).

Generalized Additive Models (GAMs) were fitted using the dsm function of the dsm R package (Miller et al. 2013). These GAMs modeled common dolphin counts per transect segment, corrected for detectability, as a function of smooths of the considered environmental variables. The model structure is as follows:

$$E(n_j) = \hat{p}_j A_j \, exp\left[\beta_0 + \sum f_k(z_{jk})\right],$$

where n_j is the count in segment j, $\hat{p}_j$ is the estimated detection probability in segment j, β_0 is an intercept term, the f_k represents the smooth function associated with covariate k and z_{jk} is the value of the variable in segment j (Miller et al. 2013). The $\hat{p}_j A_j$ term is included in the model as an offset, where $\hat{p}_j$ is the detection probability in segment j and A_j is the area of segment j. The offset is a term for which the coefficient is not estimated, but assumed to be one, allowing one to model corrected counts as the response while accounting for detectability.

Models were fitted using all transect segments and common dolphin sightings on effort. A stepwise backward selection was implemented based on AIC to select the final model. The smoothing parameter estimation method was REML. To prevent overfitting, restrictions on the maximum degrees of freedom for all variables' smooth functions were implemented ($k=4$). As recommended by Miller et al. (2013), the tweedie distribution was used for the response.

Since effort was not spatially consistent across seasons (Figure 1), especially with respect to the distance to the coast, distinct smooth functions of this variable and correlated variables tested in separate models were calculated according to the season.

Variable smooth terms contributions were calculated by removing each term, one at a time, from the final model and calculating the reduction in percentage of deviance explained. A significance level of $\alpha=0.05$ was set prior to model fitting to determine if the model's smooth terms had a statistically significant effect.

2.5 | Prediction and Variance Estimation

The final model was used to predict densities in space, using the predict function from the dsm R package. For each cell of a prediction grid, an abundance value was calculated from the environmental conditions and the cell's area (its offset). This was done for all prediction grids (each corresponding to the mid-week of a given season of each year of sampling). The abundance in each cell i in grid j is given by

$$E(N_{ij}) = A_{ij} \, exp\left[\beta_0 + \sum f_k(z_{ijk})\right],$$

where N_{ij} is the abundance in prediction grid cell i for grid j, β_0 is an intercept term, the f_k the smooth function of the covariate z and z_{ijk} is the value of variable k of prediction grid cell i for grid j (Miller et al. 2013).

The total abundance in the study area, for the jth grid, is calculated through summing the predicted abundance of all cells in the grid. Predicted densities were mapped in space using the ggplot2 and viridis R packages (Garnier et al. 2024; Wickham et al. 2024). To estimate confidence intervals and the coefficients of variation (CVs) associated to the abundance estimates, the dsm_var_gam function from the dsm R package was used.

Offshore effort was deficient in spring and winter. To avoid spatial extrapolation issues in these two seasons, predictions were restricted to coastal areas (DTC < 30 km, approximately the third quantile of DTC in the survey effort data). Therefore, abundance estimates and distribution predictions for the entire EEZ were only attempted for summer and autumn, while comparisons between these seasons and spring and winter were limited to coastal areas. To prevent unrealistic density predictions at the edge of the EEZ for summer and autumn, the maximum DTC for the prediction grids was set as the third quartile of DTC in the study area (270.556 km). This value is intermediate between the 90th percentile of DTC during effort in summer (279.956 km) and autumn (262.066 km).

3 | Results

In total, 62,392 km were surveyed. Survey effort covered extensively mainland Portugal's shelf waters, with 75% of the searched transects having taken place in waters shallower than 220 m deep. Still, with much lower intensity, offshore areas were also surveyed. Effort varied in intensity and in space seasonally, according to the boarded campaigns and environmental conditions for surveying. For all seasons, there was an extensive coastal effort. Although offshore effort occurred in all seasons, it was mostly concentrated and evenly spatially distributed during summer and autumn (Figure 1). A total of 28,771 km were covered in spring months, 9042 km during summer, 14,690 km in autumn and 9889 km in the winter.

There were 737 common dolphin sightings recorded on effort. The mean group size was 10.16 individuals (SD = 15.87), ranging from single animals to large aggregations of 200 dolphins. In general, common dolphins were mostly sighted in shelf waters, with greater aggregations on the northern-central western coast (Figure 2). The environmental conditions during sampling and where common dolphins were detected are summarized in Table 2.

3.1 | Modeling Results

3.1.1 | Detection Function

The chosen detection function considered a half-normal key and sea state as a factor covariate (Figure 3). The average detection probability was 0.493 (CV = 0.025), with effective strip width and detection probability showing variation according to sea state (Table 3).

3.1.2 | Density Surface Model

The selected density surface model included smooths of DTC (one per season), SST, CHL, Salinity, and Zooplankton (for

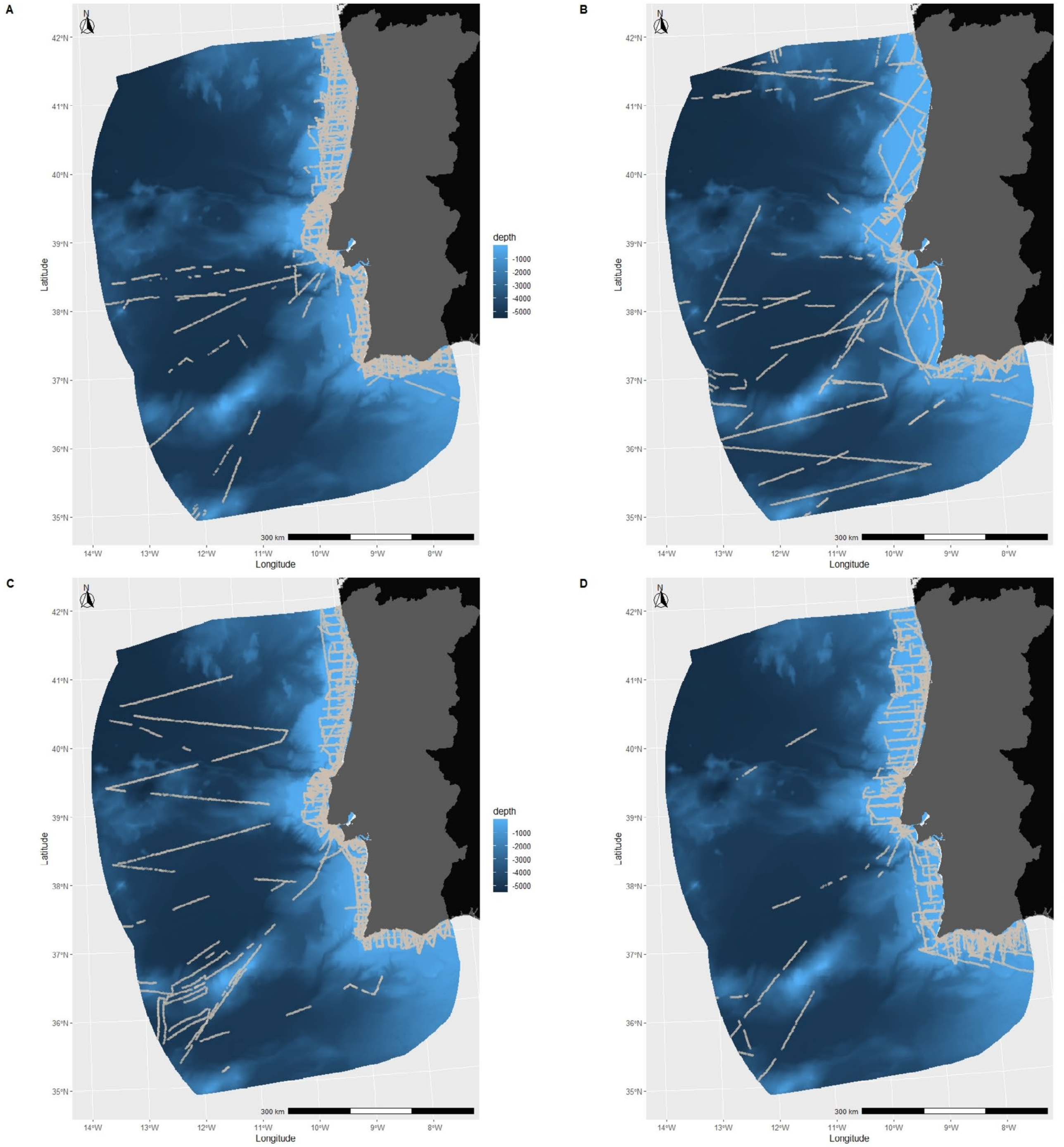

FIGURE 1 | Transect effort (light gray) across the seasons. Blue scale represents bathymetry. (A) spring effort, (B) summer effort, (C) autumn effort, and (D) winter effort.

AIC comparisons to other models refer to Table S1). All smooth terms of the variables kept in the final model had statistically significant relationships with common dolphin density, with the exception of CHL (Table 4).

The partial effects plots (Figure 4) reveal how estimated common dolphin density varies across the environmental gradient. The effect of distance to the coast varied seasonally, with the model predicting higher coastal density in the summer and winter, a density peak further offshore in the autumn, and a positive trend with distance to the coast during spring. There is a negative relationship between common dolphin density and SST, with highest density estimated in cold waters, a plateau in the smooth function between 15°C and 20°C and a significant drop in common dolphin density in waters warmer than 20°C. Contrasting this, the model predicted high common dolphin density in waters with high Salinity and Zooplankton concentrations. Finally, the response curve for CHL reveals a peak of common dolphin density when surface chlorophyll-a is between 4 and 6 mg/m^3, which are high values of surface chlorophyll-a concentration (Table 2).

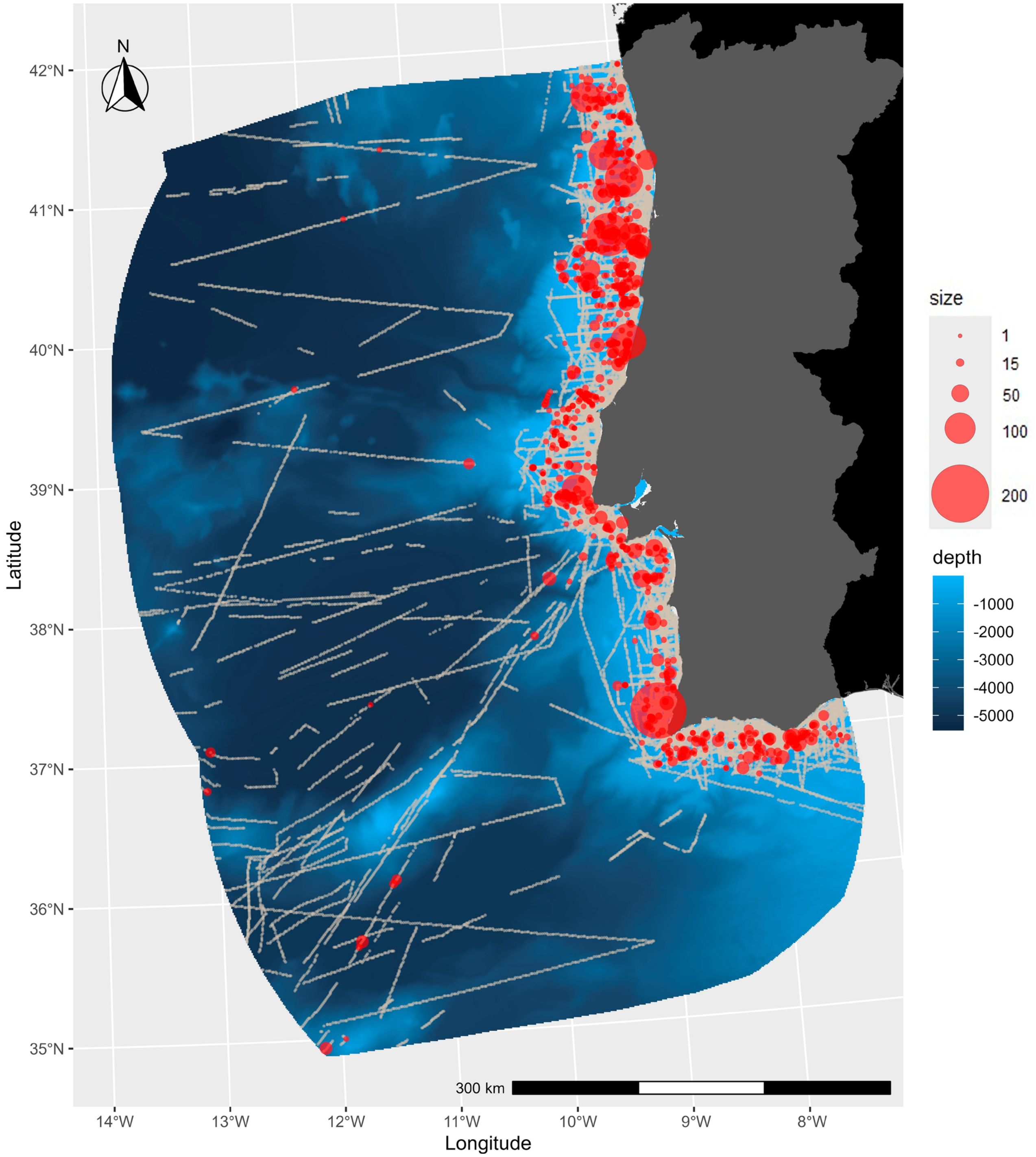

FIGURE 2 | Transect effort (light gray) and common dolphin sightings (red) recorded from 2004 to 2020 in mainland Portugal's EEZ. Point size is proportional to group size. For spatial context, Portugal shown in dark gray and Spain in black.

3.2 | Model Predictions

3.2.1 | Comparisons With SCANS Surveys

Model-based abundance and density estimates for summer 2016 (in SCANS-III blocks) and summer 2020 (in SCANS-IV blocks) were compared with their respective survey results. The model predicted lower densities than those obtained in SCANS-III, yielding estimates closer to SCANS-IV, with confidence intervals overlapping across all comparisons (Figure 5 and Table S3).

3.2.2 | Coastal Abundance and Distribution

The selected model predicted seasonal differences in abundance and distribution in the coastal region. Generally, model-based abundance estimates in coastal waters for spring were the lowest, varying from 13,737 (CV = 0.1106) in 2020 to 25,887 (CV = 0.1131) dolphins in 2016, with a median of 17,249 (CV = 0.0980) for 2005. Summer had the highest abundance estimates on the coast, ranging from 23,843 (CV = 0.1663) in 2004 to 34,340 (CV = 0.1466) individuals in 2012, with a median of 29,318 (CV = 0.1266) for

TABLE 2 | Summary statistics of the environmental conditions during sampling and where common dolphin sightings were recorded from 2004 to 2020 in mainland Portugal's EEZ.

Variable	Mean	Median	SD	Range	Temporal resolution
Depth–Sampling	−679.6	−101.5	1393.0	−5353.4–0.0	NA
Depth–Sightings	−313.6	−101.0	1391.2	−5050.1–0.0	
Slope–Sampling	1.48	0.39	2.37	0.02–16.23	NA
Slope–Sightings	1.66	0.51	2.77	0.05–16.01	
DTC–Sampling	42,844	14,588	78,059	1.4–370,794	NA
DTC–Sightings	23,670	16,705	36,965	711–366,450	
DT200–Sampling	28,108	14,159	43,121	3–322,749	NA
DT200–Sightings	16,192	10,414	18,894	4–182,113	
DT1000–Sampling	35,944	27,805	36,190	2–304,563	NA
DT1000–Sightings	25,297	23,415	18,283	7–169,332	
SST–Sampling	16.48	16.11	2.32	11.14–26.10	8D
SST–Sightings	15.88	15.65	2.04	11.99–21.70	
CHL–Sampling	1.19	0.86	1.05	0.05–9.00	8D
CHL–Sightings	1.34	1.06	1.05	0.08–5.66	
CHL–lag3–Sampling	1.18	0.72	1.16	0.05–9.00	8D
CHL–lag3–Sightings	1.32	0.88	1.15	0.05–7.32	
Salinity–Sampling	35.49	35.67	0.93	18.19–36.81	8D
Salinity–Sightings	35.52	35.62	0.56	29.31–36.47	
Zooplankton–Sampling	2.91	2.63	1.90	0.08–32.03	8D
Zooplankton–Sightings	3.43	3.06	1.97	0.48–12.62	

Note: The sampling unit is the segment.
Abbreviations: 8D, 8-day composite; NA, non-applicable; Y, yearly.

2020. Model-based autumn abundance estimates were intermediate between spring and summer, from 19,052 (CV = 0.1205) dolphins in 2009 and 34,179 (CV = 0.1309) for 2008, with a median of 22,468 (CV = 0.1157) dolphins in 2015. Winter abundance estimates were similar to autumn, ranging from 18,713 (CV = 0.1130) in 2004 to 29,664 (CV = 0.1595) in 2005, with a median of 21,492 (CV = 0.1108) for 2008. Although for all seasons the abundance estimate was mostly constant across survey time, abundance peaks were estimated punctually, without a clear temporal pattern, especially for autumn and winter (Figure 6).

The predicted spatial distribution is patchy along the coast, typically with higher estimated densities on the west coast (Figures 7 and S5–S20). Consistently, the model predicted higher common dolphin densities in the edge of the coastal region in spring and autumn, when compared to summer and winter.

3.2.3 | Portuguese EEZ Abundance and Distribution

When accounting for the entire region, only for summer and autumn, the model also predicts seasonal differences in abundance and distribution. Model-based abundance estimates for the entire Portuguese EEZ were consistently higher in the autumn than in the summer, although the associated CVs were greater and, consequently, the confidence intervals much broader in the former than the latter (Figure 8). Predicted autumn abundance varied from 97,635 (CV = 0.2303) individuals in 2016 to 194,762 (CV = 0.2621) individuals in 2008, with a median in the time series of 169,421 (CV = 0.2840) in 2012. For the summer, model-based abundance estimates varied from 62,237 (CV = 0.2709) in 2004 to 108,640 (CV = 0.2169) in 2011, with a median in the time series of 95,026 (CV = 0.2024) in 2005.

When comparing the predicted spatial distribution in the entire EEZ, there is a consistent pattern of higher densities inshore during the summer than in the autumn (Figure 9 and Figures S21–S36). The model predicts higher densities in coastal waters in the summer, with moderate densities in slope waters. Contrasting this, the predicted spatial densities are higher in slope waters in the autumn, being moderate to low in shelf waters. In both seasons, the model predicts an abrupt drop in common dolphin densities offshore.

4 | Discussion

The available data allowed a unique analysis on the long-term spatiotemporal variability of common dolphin densities across a highly hydrographically dynamic region such as the Portuguese EEZ. Our model predicts a seasonally varying patchy distribution of common dolphins in Portuguese coastal waters, consistent with Moura et al. (2012). The model also detected offshore presence, though less pronounced than coastal occurrence during summer, as reported by Gilles et al. (2023). We highlight these results were based on an opportunistic dataset. Therefore, they must be interpreted with the caution that any opportunistic dataset entails. The caveats of our data, and possible implications for the results, are further discussed at length below.

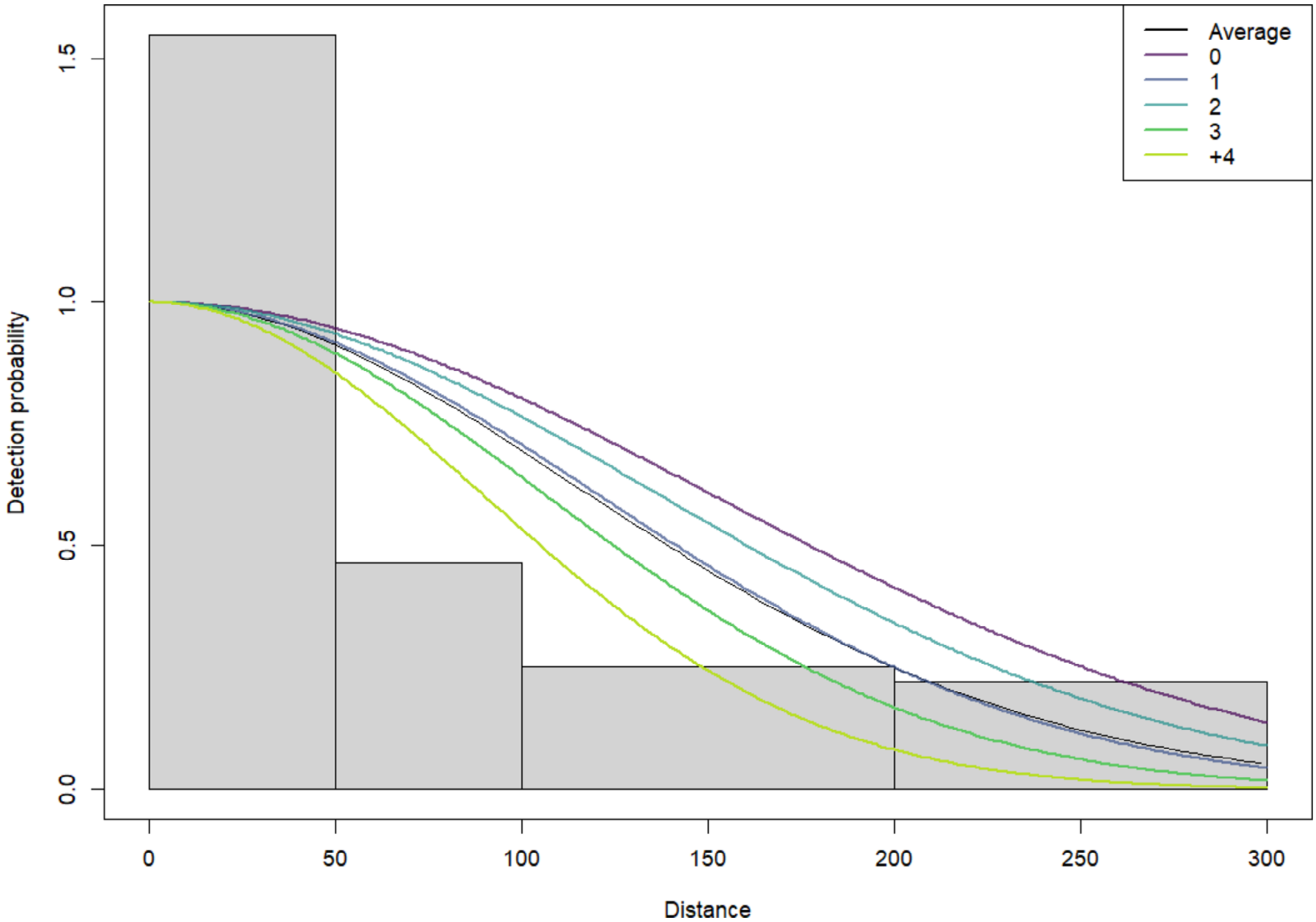

FIGURE 3 | Selected detection function (line)—with a half-normal key-function and sea state as a factor covariate (colored lines) to model common dolphin detectability—as a function of the perpendicular distance to the trackline, using data recorded from 2004 to 2020 in mainland Portugal's EEZ. Distance was recorded in four intervals: (i) 0–50 m; (ii) 50–100 m; (iii) 100–200 m and (iv) 200–300 m. Truncation distance is 300 m.

TABLE 3 | Estimated parameters of the chosen detection function.

Sea state (Beaufort)	Effective strip width (m)	Detection probability
0	180.12	0.600
1	148.86	0.496
2	166.32	0.554
3	132.25	0.441
≥4	111.90	0.373

4.1 | Model Results

4.1.1 | Environmental Variables and Spatial Distribution

The environmental variables retained by the final model, and their effects on common dolphin density, are in line with the existing literature (Fernandez et al. 2021; Gilles et al. 2023; Moura et al. 2012), leading to sensible spatial distributions.

Seasonal smooths of DTC revealed that common dolphins change their presence in coastal environments according to the season. The model predicts that during spring and autumn, common dolphins are further offshore than in summer and winter. This seasonal shift is evident in the coastal distribution maps, which show spring and autumn concentrations occur primarily at the offshore edge of the coastal zone while summer and,

TABLE 4 | Summary of variable contributions to deviance explained.

Variable	*p*	% Contribution
s(DTC, by = Season)	Season = spring; $p \leq 0.001$ Season = summer; $p \leq 0.001$ Season = autumn; $p \leq 0.001$ Season = winter; $p = 0.0033$	58.74%
s(SST)	$p \leq 0.001$	14.62%
s(Zooplankton)	$p = 0.0010$	10.79%
s(Salinity)	$p = 0.0405$	3.01%
s(CHL)	$p = 0.0504$	6.01%

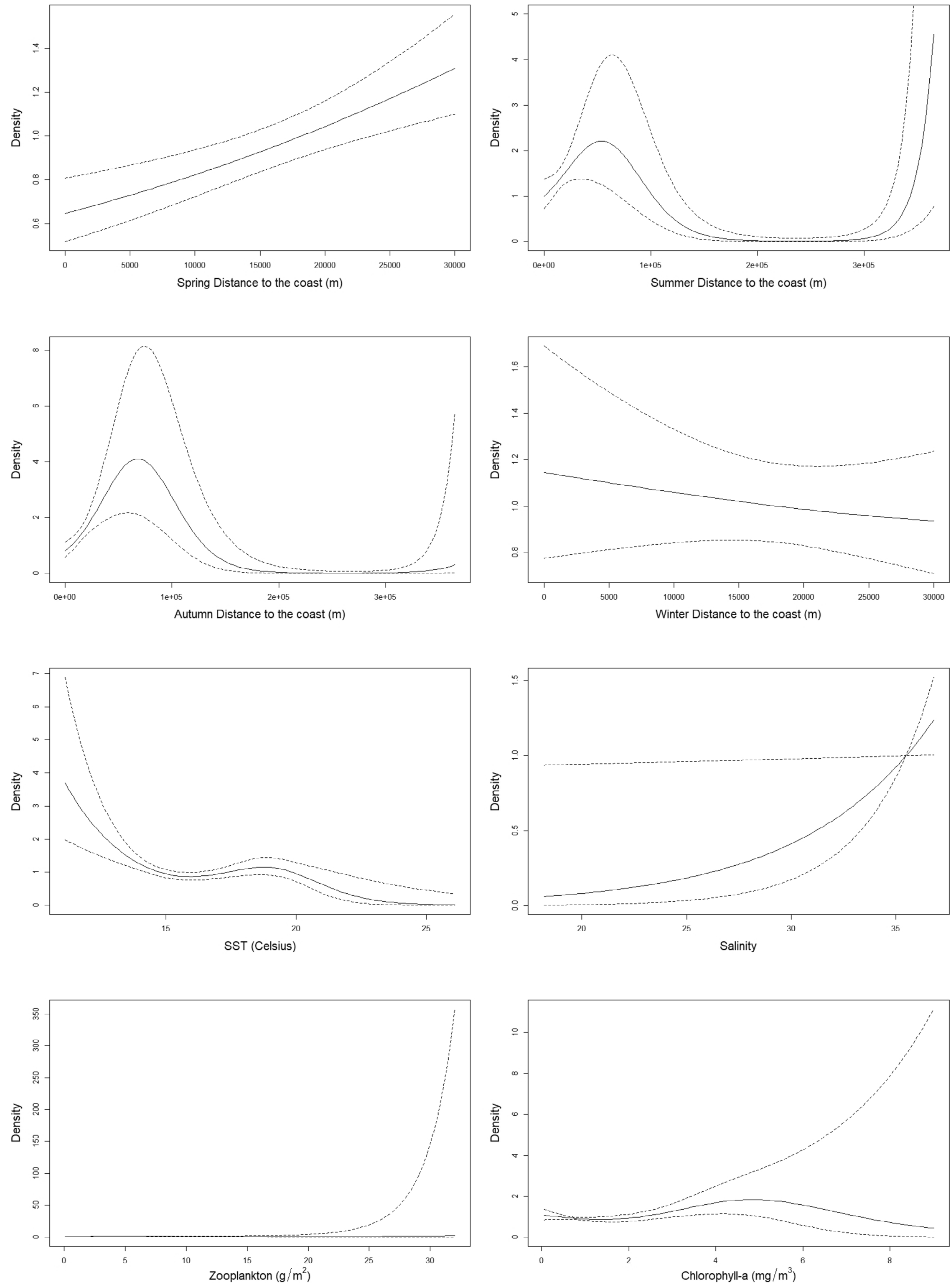

FIGURE 4 | Legend on next page.

FIGURE 4 | Partial effects plots for each covariate, showing how the estimated common dolphin density varied according to the environmental gradient. Solid lines show the mean and dotted lines limit the standard error bands. In particular, for Zooplankton, for which the form of the estimated smooth is obscured by the low precision, we refer to Figure S2 in the Supporting Information, where smooths are represented without the corresponding standard errors, providing a more informative view of the corresponding relationships.

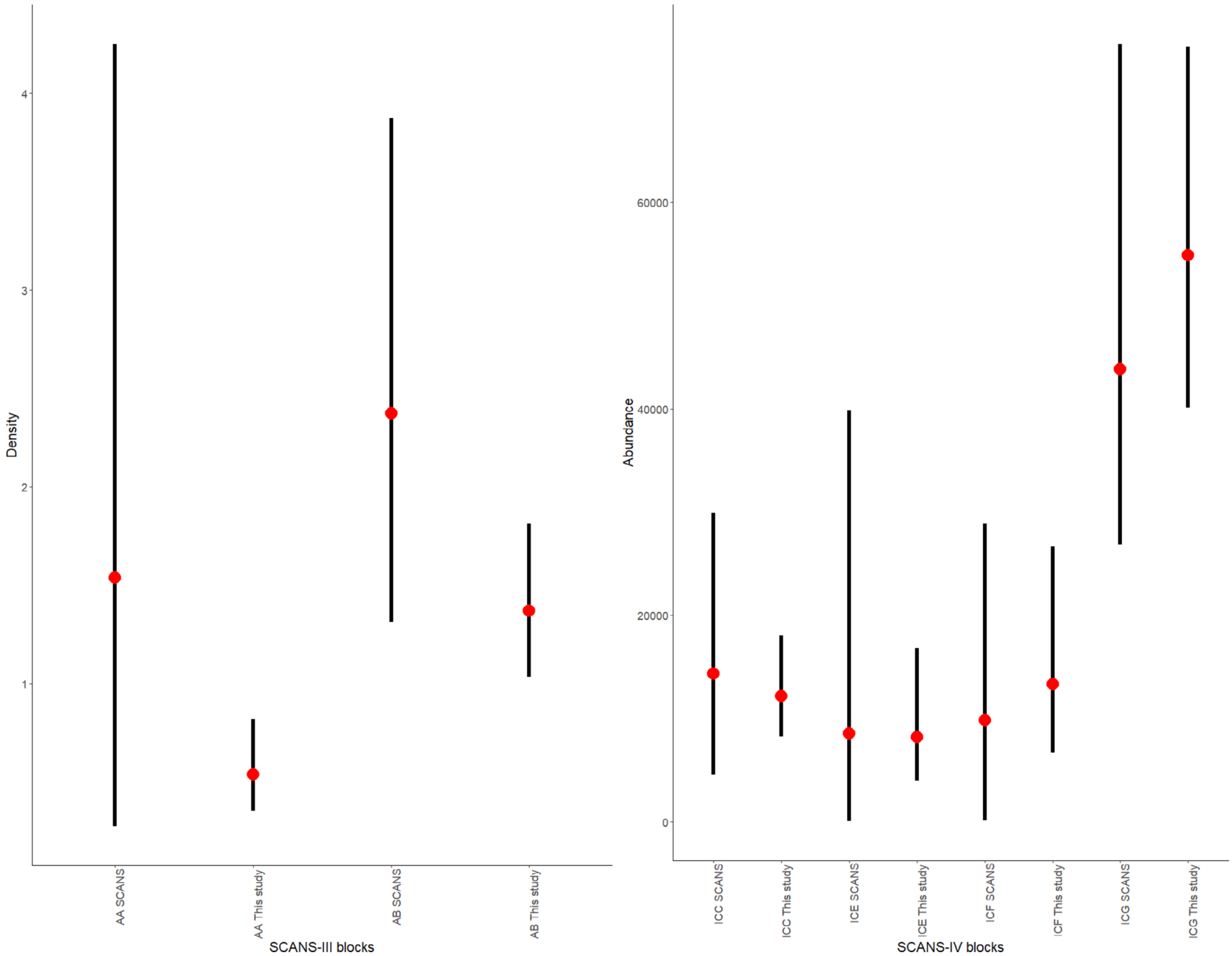

FIGURE 5 | Comparison between SCANS-III—left—(Hammond, Lacey, et al. 2021) reported densities and SCANS-IV surveys—right—(Gilles et al. 2023) reported abundances with final model predictions in their respective blocks. Red points represent point estimates and lines represent the confidence intervals. Since SCANS-III blocks overlap with the Spanish coast, instead of absolute abundance, average density and associated confidence intervals for SCANS-III blocks are compared with their overlapping area with this study's study area. Model-based abundance estimates for SCANS-IV blocks were done for summer 2020, the year in our dataset closest to the SCANS-IV survey. For detailed model-based abundance estimates, refer to the Table S3.

to a lesser extent, winter predictions show greater aggregations distributed throughout the inner coastal environment. Further, there are latitudinal distribution differences between spring and autumn. In spring, the model generally predicts higher common dolphin densities in the south of the coastal region than for the autumn, where densities in the north are generally higher. Within the Portuguese EEZ, the model predicts seasonal shifts in density related to DTC, with peaks occurring inshore during summer and in offshore slope waters during autumn.

Differences in spatial distribution may be related to seasonal shifts in prey availability in coastal environments. It is possible that when prey species are not as concentrated in the coastal region, dolphins move further offshore in search of food. A similar seasonal pattern has been described for sardines' spatial distribution in Portuguese shelf waters. Potential habitat for sardines in the spring is concentrated in the southern portion of the coast, shifting northwards in the autumn (Zwolinski et al. 2010). Data limitations for summer and winter prevented us from relating sardine distribution and observed dolphin spatial patterns during these seasons.

Nonetheless, sardine body condition in Portuguese shelf waters is highest at the end of the summer, and spawning activity

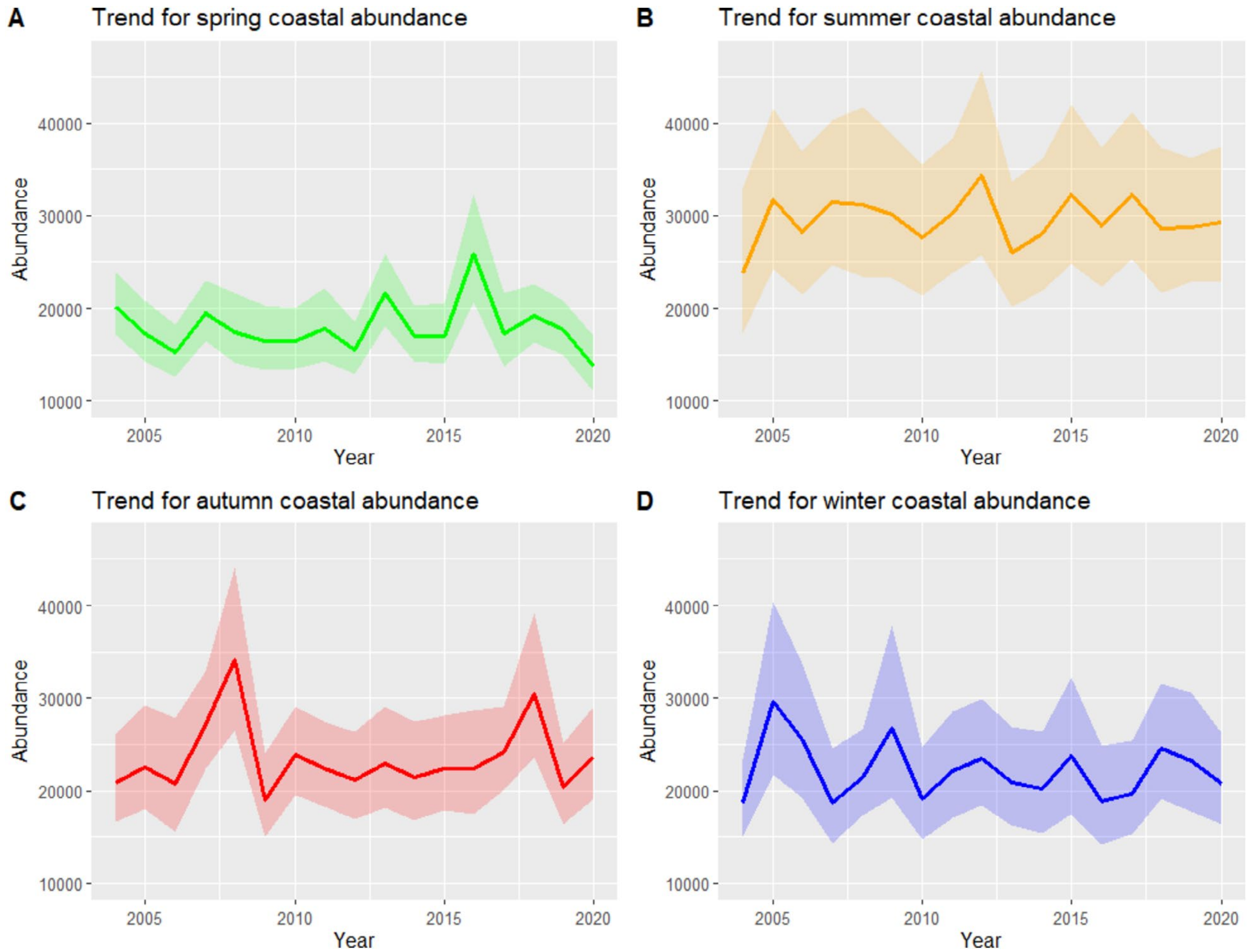

FIGURE 6 | Interannual variation in model-based abundance estimates for common dolphins according to the season: (A) spring, (B) summer, (C) autumn, and (D) winter. Solid lines show the point estimates and the colored ribbons represent the 95% confidence intervals for the abundance estimates. For detailed model-based abundance estimates, refer to the Supporting Information.

reaches its maximum during the winter (Silva et al. 2008). While differences in common dolphin density and occurrence relative to DTC have not been directly related to prey availability at a seasonal scale, dolphins have been found to concentrate further offshore in years when sardine biomass in shelf waters is lower (Brouder et al. 2025). Therefore, the occurrence of seasonal dolphin movements in and out of coastal environments in search of prey is also possible. The summer mating season in Eastern North Atlantic common dolphins (Murphy et al. 2005) could serve as an additional explanation for the model predicting higher density closer to the coast during this season. Mother-calf pairs may seek refuge from potential predators, like large sharks, by being close to the coast, as seen in dusky dolphins (*Aethalodelphis obscurus*; Weir et al. 2008) and Risso's dolphins (*Grampus griseus*; Hartman et al. 2014). The combined effects of prey availability and breeding behavior may explain why the predicted distribution is more concentrated in coastal environments in summer than in autumn. Dolphins likely move to shelf waters in summer, targeting sardines with higher body condition while protecting their calves from potential predators, then venture offshore in autumn looking for prey.

The retained dynamic variables (SST, CHL, Salinity and Zooplankton) were used as proxies for the distribution of dolphin prey which might be causal with respect to the dolphin distribution. The model predicts higher common dolphin density in colder waters (below 20°C), with high chlorophyll-a and zooplankton concentrations, variables associated to sardine's diet (Garrido et al. 2008). This concurs with the common dolphin distribution patterns detected in other parts of the globe. Common dolphins in both the Eastern Tropical Pacific and the Eastern North Atlantic have been found to be associated with colder waters, rich in nutrients (Au and Perryman 1985; Fernandez et al. 2021; Sousa et al. 2023). This suggests that these oceanographic conditions may broadly reflect preferred foraging habitats across their range—a pattern that appears to hold true here as well. Association with cold waters and high productivity can also be related with the Western Iberian coastal upwelling system. Strong winds push seawater offshore, leading to deep, cold and nutrient-rich water to rise towards the surface (Chabrerie and Arenas 2024). It is possible, therefore, that common dolphin density is somewhat dependent on coastal upwelling, as it creates favorable conditions for sardine occurrence—low SST (Lima et al. 2022)—and growth—by increasing phytoplankton concentrations, which sardines feed on (Garrido et al. 2008). Interestingly, our model did not retain a chlorophyll-a time lag of 3 months, rather retaining the concentration for the week of the sighting. This

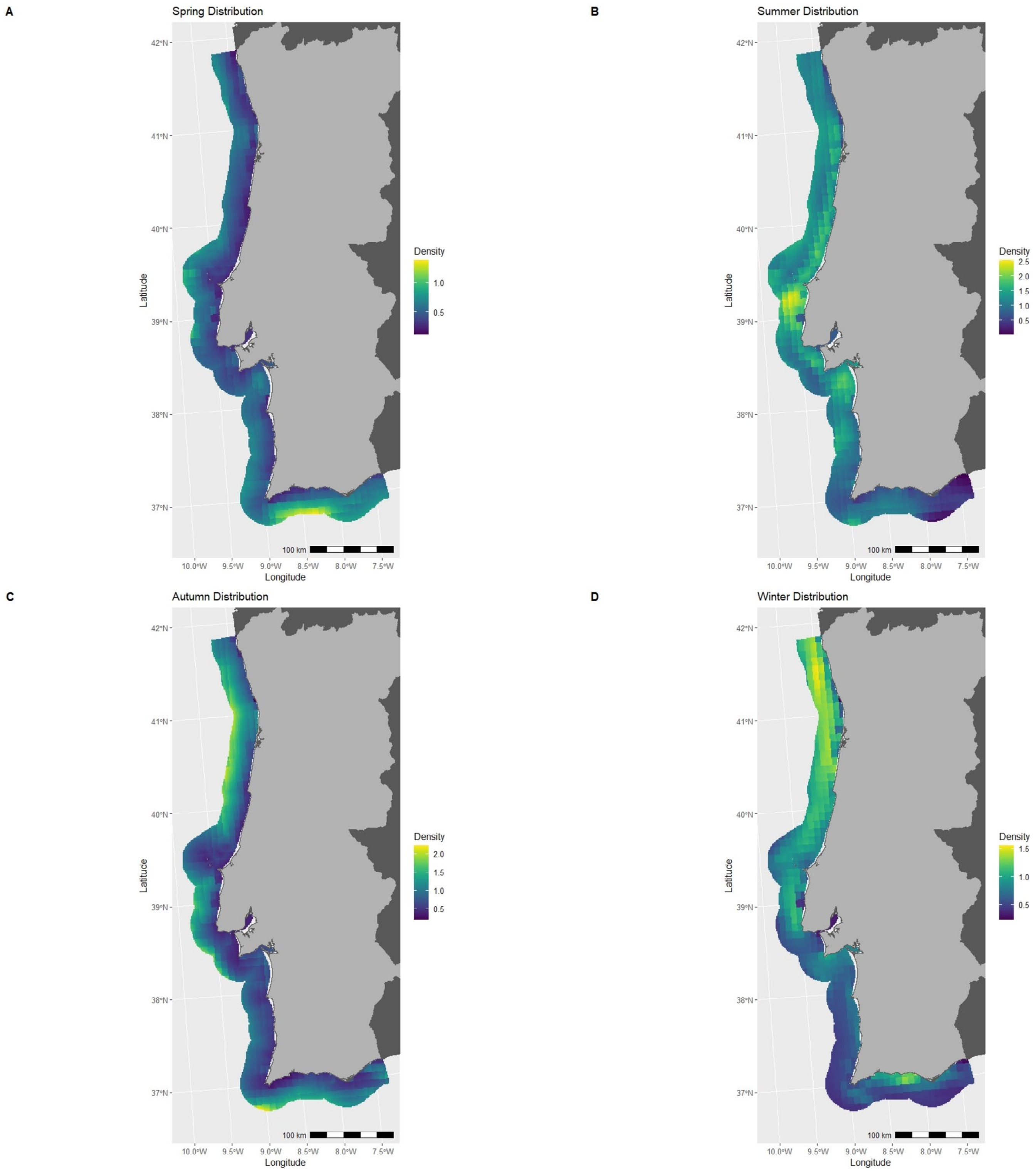

FIGURE 7 | Predicted common dolphin density distribution in Portuguese coastal waters for 2020 (the most recent year in the time series), according to the season: (A) spring, (B) summer, (C) autumn, (D) winter. See the Supporting Information (Figures S5–S20) for predictions for 2004–2019. Coastal areas are defined as the region where DTC < 30 km.

can be explained by sardine's phytoplankton rich diet, especially in the Portuguese west coast (Garrido et al. 2008). Since sardines feed mostly on phytoplankton, they should aggregate in areas where chlorophyll-a concentration is higher, and the dolphins will follow them there. This corroborates our model results, and they suggest that common dolphins aggregate in high primary productivity events when they are happening, following their preferred prey items, and then might move on in search of new prey aggregations. Still, sardines also feed on zooplankton (Garrido et al. 2008), which is another variable retained in the final model. The model predicts higher common dolphin density when zooplankton is highest. The partial

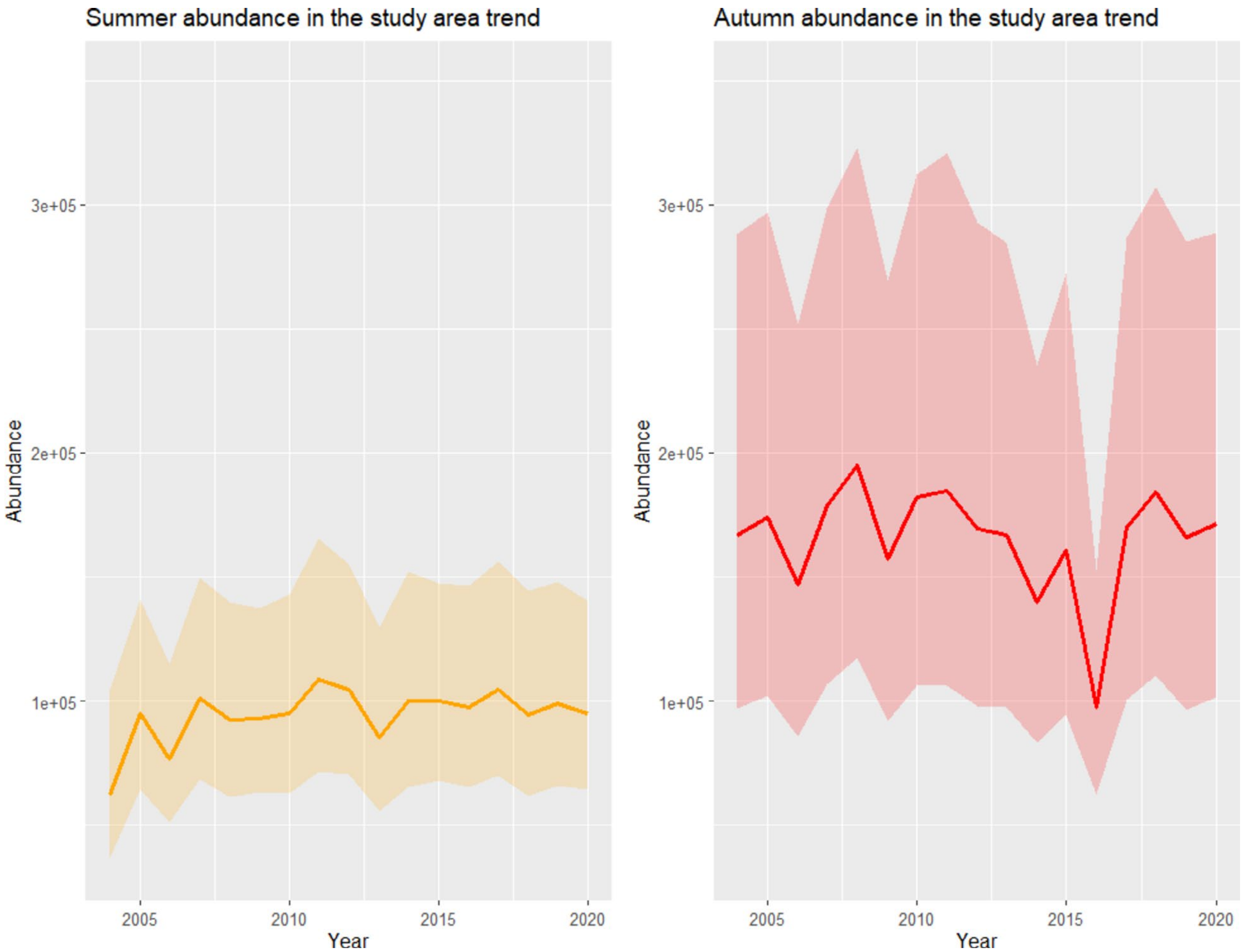

FIGURE 8 | Interannual variation in model-based abundance estimates for common dolphins according to the season: Left—summer and right—autumn. Solid lines show the point estimates and the colored ribbons represent the 95% confidence intervals for the abundance estimates. For detailed model-based abundance estimates, refer to the Supporting Information.

effects of CHL and Zooplankton, therefore, suggest that common dolphins aggregate in areas where their prey may find ample amounts of food, which will likely be areas where prey availability is also highest. Additionally, the positive relationship between common dolphin density and salinity, combined with a preference for colder waters, matches the habitat preference of the sardine, which has been found to prefer a water temperature below 20°C and high sea surface salinity (Lima et al. 2022).

4.1.2 | Comparisons With SCANS Surveys Abundance Estimate

This study used an opportunistic dataset to model common dolphin spatial densities. Poorer data quality when compared to dedicated marine mammal distance sampling survey data could suffer from detectability issues which can lead to unreliable abundance estimates. Limitations concerning data collection and the detection process are discussed at length in the Assumptions and limitations section below. Still, to understand how well our model predicted common dolphin abundance, we compared abundance estimates with those obtained in the SCANS-III and SCANS-IV surveys (Gilles et al. 2023; Hammond, Lacey, et al. 2021).

All the confidence intervals (CIs) we produced, either for abundance or for mean density, overlapped greatly with those reported for either SCANS surveys (Gilles et al. 2023; Hammond, Francis, et al. 2021). While this is a good sign that our model can produce sensible abundance estimates, the CIs overlap reflects also how wide these are, reflecting overall low power to eventually detect existing differences. Despite the CI's overlap, our density estimates for the SCANS-III blocks in the summer of 2016 were much lower than those originally reported, 65.08% smaller than the reported value for the AA block and 42.46% smaller than the reported value in the AB block. Comparisons with the SCANS-IV survey yielded more comparable results. Point estimate differences between our model and the SCANS-IV results ranged from 4.25% for the ICE block to 35.30% for the ICF block. Overall, we consider that our model predicts abundances for the SCANS survey blocks similar enough to what had been previously reported. Therefore, our analysis can bring forth sensible abundance estimates, although the large differences in the SCANS-III blocks caution us against focusing on their absolute values, especially for management and conservation decisions. Instead, we suggest that focus should be kept on the seasonal and interannual trends.

These comparisons require caution. Our density and abundance estimates for SCANS survey blocks are not directly

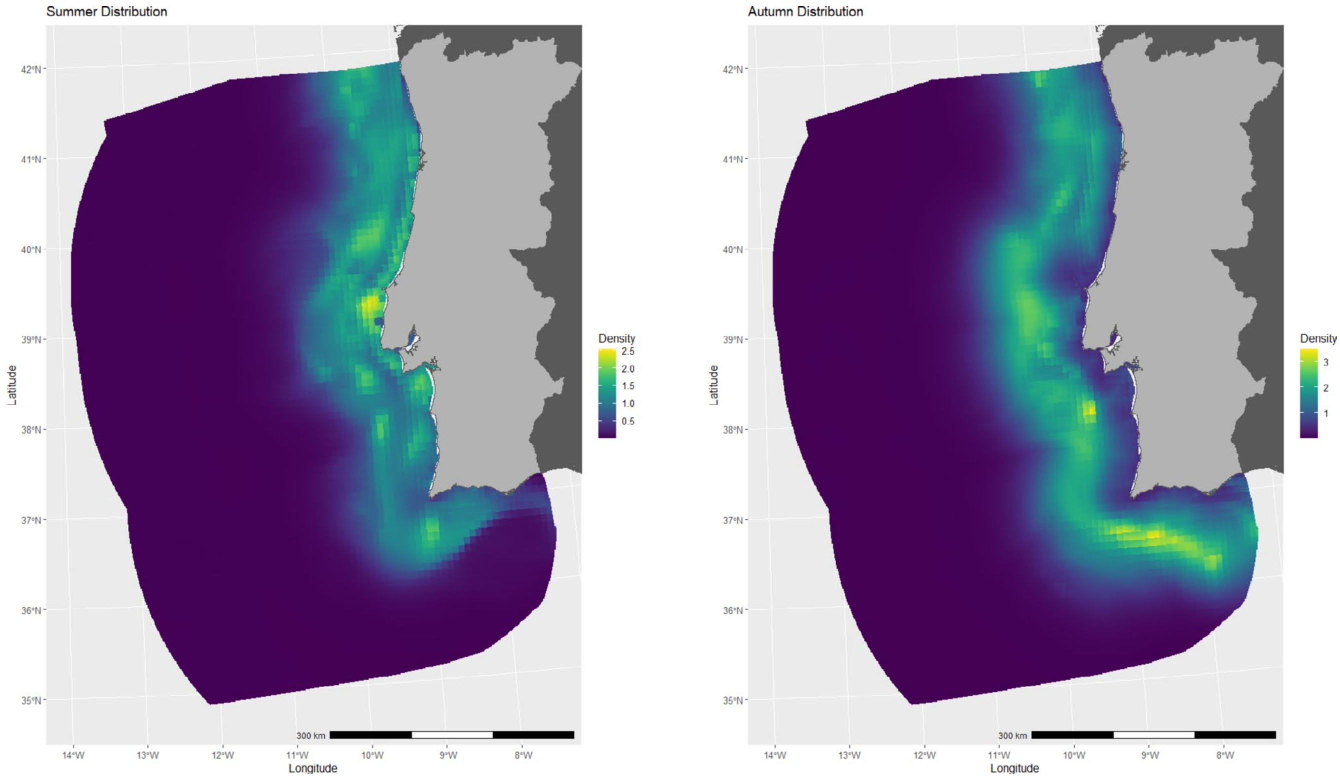

FIGURE 9 | Predicted common dolphin density distribution in the entire Portuguese EEZ for 2020 (the most recent year in the time series), according to the season: Left—summer, right—autumn. See the Supporting Information (Figures S21–S36) for predictions for 2004–2019.

comparable to published values. The SCANS-III AA and AB blocks extend into Spanish shelf waters beyond our study area; we compared only the portions within mainland Portugal's EEZ to values reported by Hammond, Lacey, et al. (2021). For this to be a valid direct comparison, one would have to assume uniform dolphin distribution within blocks, which would be optimistic at best. For SCANS-IV, surveyed in summer 2022 (Gilles et al. 2023), we predicted into summer 2020 as the latest available period within our data, assuming similar environmental conditions between years. Both comparisons should be interpreted cautiously.

4.1.3 | Seasonal and Interannual Abundance Estimates and Associated Uncertainty

Seasonal coastal abundance estimates varied greatly, with the highest values occurring during the summer and the lowest in spring. Autumn and winter estimates were intermediate. CIs were widest, not surprisingly, in summer, when coastal effort was lowest, though differences in uncertainty across seasons were minor. Interannual variation in coastal abundance was not large, despite occasional peaks, with the seasonal pattern remaining relatively constant throughout the study period.

These seasonal differences in coastal abundance are consistent with the spatial distribution patterns and environmental drivers discussed in Section 4.1.1, particularly the combined effects of prey availability and reproductive behaviour.

Abundance estimates for the entire Portuguese EEZ also varied seasonally, being much greater in the autumn than in the summer. We attribute this difference to higher densities in offshore waters in the autumn, despite the lower abundance in the coastal region when compared to the summer. Similarly to the coastal environment, this pattern remained consistent throughout the years, besides a low in predicted abundance in the autumn of 2016. Despite the large difference in point estimates, the CIs between summer and autumn abundance in the EEZ greatly overlapped due to the large uncertainty associated with the autumn point estimates. Looking into the seasonal response curve for DTC, uncertainty in estimated density increases greatly far offshore in the autumn, explaining the wide CIs. While it is possible that large numbers of common dolphins could move from adjacent areas into Portuguese offshore waters during the autumn, explaining why estimated abundance is much greater in the autumn than in the summer, we consider that the uncertainty in autumn abundance lowers one's ability to interpret such discrepancies. Establishing whether such large differences between summer and autumn abundance of common dolphin in Portuguese waters are real would rely on additional data, in particular, higher effort in offshore regions.

4.2 | Common Dolphin Conservation and Management Insights

Our model strongly suggests that variables related to sardine optimal habitat and growth are behind the ecological process underlying common dolphin density distribution. In a climate change scenario, where the average SST expected to increase from 1.2°C to 3.2°C by 2100, depending on the scenario considered, (Genner et al. 2017), the colder water dependent sardines are expected to have a northward shift in distribution (Lima et al. 2022). This would result in lower prey availability for mainland Portugal's common dolphins, which preferably target sardines (Marçalo et al. 2018). Consequently, a northward shift in common dolphin distribution might be expected due to climate change, supported by our model results and the literature (MacLeod 2009; Sousa et al. 2023). However, climate change effects can be hard to predict as global warming could lead to the opposite effect by intensifying coastal upwelling in the Western Iberian coast (Sousa et al. 2017), leading to greater primary productivity. This could, in turn, create more favorable conditions for sardine occurrence and growth. On the other hand, more recent studies have shown that despite the enhancement of upwelling favorable wind patterns with climate change, the increase in SST is expected to increase upper water layer stratification, hampering the rise of cold, nutrient-rich waters towards the surface, leading to a less effective coastal upwelling system (Sousa et al. 2020). The complexity of climate change interactions with oceanographic conditions makes it especially hard to predict climate change impacts on top predators.

Regardless of the potential climate change impacts on prey abundance, distribution and, consequently, on common dolphin density, they may be exacerbated by human activity, especially overfishing, reducing even further the available sardine biomass, leading to the potential reduction of common dolphin density in the region. This interpretation does not account for the dolphin's adaptability. Cetaceans are highly adaptable, and common dolphins in Galician waters, adjacent to our study area, have been found to shift their main prey items in response to prey availability (Santos et al. 2013). Nevertheless, this is contrary to what has been reported for mainland Portugal (Marçalo et al. 2018), and our results also support a link between common dolphin density and environmental conditions favorable to sardine occurrence and growth. Therefore, the sustainable management of sardine stocks is likely to be a key consideration for conserving the common dolphin population in this region. Importantly, this underscores the need for a more inclusive approach to fisheries management, one that considers not only the health of the stock and the fisheries' socioeconomic needs but also the ecological roles that species like sardine play in the marine ecosystem. By integrating ecological knowledge into policy decisions, we can help align fisheries practices with conservation goals (e.g., Sánchez-Jiménez et al. 2019) and avoid further impacts on the dolphins' main food resources.

4.3 | Assumptions and Limitations

Our inferences, as any model-based inferences, rely on a set of assumptions. Here we discuss the implications of these assumptions, and their potential failure. Data collection was primarily dedicated to seabirds, not marine mammals. Most common dolphin sightings (385 out of 737) occurred in the first distance bin, 0–50 m perpendicular distance from the trackline, with a significant decrease in detections in the following bands. This may be not just a result of detectability. On the one hand, observers might sometimes only detect animals after they moved towards the vessel. On the other, the use of one sided transects might have led to an artificial increase of the number of detections. Such protocol is not recommended for distance sampling surveys, given the difficulty in deciding whether observations on or near the line are inside or outside the covered region. A natural unconscious bias, driven by the desire of observers to not throw away data, might lead to recording these ambiguous detections more often than would be justifiable. Both of these would lead to an artificial increase in the number of detections in the first bin (e.g., Buckland et al. 2001), with a knock on effect of density estimates becoming biased high (Buckland et al. 2001). Considering common dolphin behavior (Würsig et al. 1998), it is possible that some animals had moved from one side of the line to the other, being recorded in the first bin, hence making the estimated detection function drop steeply. Given that data were binned, with only 4 bins available, model complexity, and model assessment, were necessarily limited. Exact distances are preferable for detection function modeling and model assessment, and we recommend that future studies aim to collect those. We tried to mitigate this issue by selecting the detection function primarily based on the expected shape of the detection process, instead of solely relying on process agnostic model fitting metrics like AIC. Using AIC blindly would select a detection model with a “spike” at the origin, hence that predicts much higher detection closer to the trackline, Table S2 and Figure S4, and a fast, unrealistic drop in detectability away from the line. This would lead to an underestimation of the detection probability, and a corresponding overestimation of density. On the other hand, using what we know about what the detection process might be tends to “cut across” that spike in the data, which is very likely to be closer to the true detectability, and hence providing more reliable density estimates.

Our comparisons with the SCANS survey results showed a significant overlap in CIs within all compared blocks, and our model-based point estimates for abundance in the SCANS-IV blocks were sensible. This increases our confidence in the chosen detection model. Therefore, it is likely that by focusing on the plausibility of the shape of the detection process we mitigated at least some of the impacts of potential unaccounted responsive movement. Still, as discussed above, these are not perfect comparisons, as for SCANS-III we couldn't compare the entire extent of each block and our data did not match temporally the SCANS-IV survey. Hence, we consider that the focus of this study should be on the ecological trends we observed, rather than the reported absolute abundances.

The heterogeneity in data collection effort in space conditioned our analysis. If the spatial coverage had been comparable across years, adding a time related variable in our model could help more reliably identify abundance variation between years. As established in the literature (Fernandez et al. 2021; Gilles et al. 2023; Moura et al. 2012) and as our results show, common dolphins prefer coastal areas. Moreover, in some years, effort was restricted in more coastal areas than in others. Therefore, if we included Year as a variable in our model, we could risk confounding between effort in optimal common dolphin habitat and interannual variation of common dolphin densities. By not incorporating Year in our model, the interannual differences in abundance we report here are being generated by shifts in the environmental conditions within the study period, not necessarily reflecting actual shifts in common dolphin population size.

To overcome this limitation, carefully designed surveys should be carried out in a more homogeneous way, to more easily monitor common dolphin abundance trends in the region. Following this rationale, increasing offshore effort would greatly improve our understanding of how common dolphins use the entire Portuguese EEZ. Homogeneous data collection offshore would help decrease the uncertainty in abundance estimates for autumn in the entire study region. Moreover, this would bring valuable insights into the abundance and distribution of the species in offshore waters, filling in the seasonal gaps left in this study.

Ecological interpretation of the density surface model relations should be made with care. DSMs, as SDMs (Species Distribution Models), are correlative by nature (Sillero et al. 2021). Their results do not necessarily reflect causal relationships between an animal's distribution/density and the environmental variables used for modeling (Franks et al. 2025). Therefore, while the relationships here reported are ecologically sensible, they are not necessarily the result of cause and effect. The primary driver of common dolphin density and distribution, and of top predators in general, is likely to be prey availability. As referred to above, the environmental variables used for modeling serve as abiotic proxies of prey aggregation, from which we try to infer ecological processes underlying the target species density distribution. Still, these models can be very useful for predictions, and hence management and conservation, even if the causal processes are not understood (Franks et al. 2025).

Ideally, we would have spatially and temporally explicit products of prey biomass or aggregations, similar to the products used for all other covariates. As of the writing of this paper, there are no such publicly available products for Iberian waters. This limits our understanding of how fish species, sardines in particular, impact common dolphin distribution. If such products existed, and we were able to model common dolphin density in relation to prey species biomass distribution, our density and distribution predictions might become more ecologically sensible, better reflecting real common dolphin abundance trends and distribution. The advantage of a density surface model is that if said information would become available in the future, we could repeat the analysis, adding spatially explicit sardine information in the model instead of just relying on proxies.

Incorporating spatially explicit prey availability in a model with proxies could help improve the deviance explained. Our selected model only explains 7.32% of the deviance within our data. We find it plausible that a variable like spatial prey availability could help the model better capture the ecological process underlying common dolphin density. Besides that, spatially varying upwelling indexes could also help approximate prey distribution. Smooth terms of linear combinations of environmental variables derived from PCAs have increased deviance explained in other studies (e.g., Virgili et al. 2024). While this strategy might improve model performance metrics, it reduces the interpretability of the model response curves, thus obscuring the understanding of ecological processes. Nevertheless, the low deviance explained is partially driven by the disproportionate number of transect segments without observations when compared to those with dolphin detections (737/48,875 = 1.5%). Zero inflated data are hard to model and typically lead to large errors, even when using flexible distributions like the tweedie. If transect segment area was increased, decreasing the proportion of zeros, deviance explained would increase, but this would come at a cost of lower spatial resolution, preventing a fine-scale analysis.

Finally, the environmental variables used to model marine species distributions and abundances tend to come from oceanographic models (e.g., this study; Fernandez et al. 2021; Virgili et al. 2024). This means that what we use for modeling is not a direct measurement of the environmental variable in situ, but the result of a model itself. That means, to begin with, that values which are estimated are taken as truth, and the variability of those predictions is rarely ever properly propagated to the final density estimates. Moreover, some models will be more reliable than others for a given study area. We extracted the spatially explicit dynamic environmental variables from three models (Table 2). Two were regional models, one concerning ocean physics in the Northeast Atlantic (Atlantic-Iberian Biscay Irish- Ocean Physics Reanalysis) and the other was a biogeochemical model (Atlantic-Iberian Biscay Irish-Ocean BioGeoChemistry NON ASSIMILATIVE Hindcast). The final model, used for extracting the mass content of zooplankton in the water surface, was a global model (Global ocean low and mid trophic levels biomass content hindcast). For a regional area like ours, regional models would be desirable better reflecting local processes. Due to a lack of regional information on zooplankton content in the water, which is likely related to common dolphin prey aggregations, we extracted its values from the available global model. Therefore, we consider the estimated relationship between common dolphin density and this variable to be less reliable than those estimated for the variables obtained from the regional models, as we suspect that local uncertainty should be greater in global models compared to regional ones.

Furthermore, the spatial resolution of the environmental variables may not always be the same as that of the sampling/modeling unit, in this case, the transect segments. Our segments and prediction grid cells were of a finer resolution than that of the dynamic environmental variables raster files. Therefore, some level of interpolation was required, adding unaccounted uncertainty. This can be avoided if transect segments are created after checking the environmental variables' spatial resolution. However, that was not a possibility in our study. Transect segments were, as per the opportunistic data collection protocol, predetermined to be split after every 5 min of search effort, regardless of distance traveled. Consequently, segment length varied, leading to the need for some spatial interpolation. We attempted to minimize interpolation issues by choosing reliable products with the finest spatial resolution possible, covering the sampling period, setting them all at the same spatial resolution. Future endeavors focused on propagating environmental variables' uncertainty into correlative models are, therefore, recommended, as they will help create better and more robust uncertainty measures associated with abundance point estimates.

4.4 | Conclusions and Outlook

Despite the opportunistic nature of the dataset, the relationships we established between the considered environmental variables and common dolphin density agree with the available literature on the species ecology in the study area and proximal regions (Fernandez et al. 2021; Gilles et al. 2023; Marçalo et al. 2018; Moura et al. 2012). Our findings reveal how dolphin density and distribution vary across seasons and years, offering new insights into the species' temporal ecology, particularly in offshore environments (summer and autumn) and during winter periods when survey efforts are typically constrained (Gilles et al. 2023; Virgili et al. 2024).

While detectability limitations require focusing on trends rather than absolute abundances, this study fills critical knowledge gaps in our understanding of common dolphin ecology across previously understudied spatiotemporal scales. By investigating these predator–prey relationships via proxies and seasonal patterns, we provided essential baseline information for marine ecosystem management and conservation planning. The integration of this long-term dataset with dedicated marine mammal survey data presents exciting opportunities to combine extensive temporal coverage with standardized detection protocols and, therefore, mitigate some of the detectability issues. This work demonstrates how comprehensive datasets (even if opportunistic) can reveal fundamental ecological processes, opening new perspectives on marine mammal habitat use and the dynamic nature of pelagic ecosystems in response to environmental variability.

Author Contributions

Miguel P. Martins: conceptualization, data curation, formal analysis, investigation, methodology, visualization, writing – original draft. **Marc Fernandez:** conceptualization, data curation, investigation, resources, formal analysis, supervision, writing – review and editing. **Ana Marçalo:** investigation, writing – review and editing. **Nuno Oliveira:** conceptualization, data curation, funding acquisition, writing – review and editing. **Tiago A. Marques:** conceptualization, data curation, investigation, resources, formal analysis, supervision, funding acquisition, writing – review and editing.

Acknowledgments

The authors would like to acknowledge all of SPEA's observers who collected data, without them, this paper would not have been made. ESAS data is openly available at ICES Data Portal—https://www.ices.dk/data/data-portals/Pages/European-Seabirds-at-sea.aspx. M.P.M. and T.A.M. thank financial support by CEAUL (funded by FCT—Fundação para a Ciência e a Tecnologia under the projects UID/00006/2025 and UID/00006/2023). Most of the data collection was performed within several projects co-funded through the LIFE Programme (a funding instrument for the environment and climate action from the European Commission), the Interreg Atlantic Area (by European Commission), the European Maritime and Fisheries Fund (EMFF) in Portugal (Mar2020), the Fundo Biodiversidade and the Fundo Ambiental (both from the Portuguese government), namely LIFE IBAS Marinhas (LIFE04 NAT/PT/000213), FAME (2009-1/089), LIFE MarPro (LIFE09 NAT/PT/000038), LIFE Berlengas (LIFE13 NAT/PT/000458), MedAves Pesca (MAR-01.04.02-FEAMP-0023), and LIFE Ilhas Barreira (LIFE18/NAT/PT/000927). CCMAR is thankful to projects UIDB/04326/2020, UIDP/04326/2020 and LA/P/0101/2020. The authors thank the Editors and two anonymous Reviewers for providing valuable comments and suggestions, which greatly improved this work. Open access publication funding provided by FCT (b-on).

Funding

This work was supported by Fundação para a Ciência e a Tecnologia (UID/00006/2025, UIDB/00006/2020).

Conflicts of Interest

The authors declare no conflicts of interest.

Data Availability Statement

The processed data that support the findings of this study, together with the code to analyze it, are openly available in Zenodo https://zenodo.org/records/18711398. Raw data can be found in the ESAS/ICES data portal https://esas.ices.dk/inventory.

References

ArcGIS Hub. 2024. "World Exclusive Economic Zones Boundaries." https://hub.arcgis.com/maps/17da5ddd3bff4d1fbc13199194491de0/about.

Au, D. W. K., and W. L. Perryman. 1985. "Dolphin Habitats in the Eastern Tropical Pacific." *Fishery Bulletin* 83, no. 4: 623–643.

Bakun, A., B. A. Black, S. J. Bograd, et al. 2015. "Anticipated Effects of Climate Change on Coastal Upwelling Ecosystems." *Current Climate Change Reports* 1, no. 2: 85–93. https://doi.org/10.1007/s40641-015-0008-4.

Bedriñana-Romano, L., P. M. Zarate, R. Hucke-Gaete, et al. 2022. "Abundance and Distribution Patterns of Cetaceans and Their Overlap With Vessel Traffic in the Humboldt Current Ecosystem, Chile." *Scientific Reports* 12, no. 1: 10639. https://doi.org/10.1038/s41598-022-14465-7.

Brouder, S., T. A. Marques, N. Oliveira, P. Monteiro, J. M. S. Gonçalves, and A. Marçalo. 2025. "When Sardines Disappear: Tracking Common Dolphin, Delphinus Delphis, Distribution Responses Along the Western Iberian Coast." *Animals* 15, no. 11: 1552. https://doi.org/10.3390/ani15111552.

Buckland, S. T., D. R. Anderson, K. P. Burnham, J. L. Laake, D. L. Borchers, and L. Thomas. 2001. *Introduction to Distance Sampling*. Oxford University Press.

Carretta, J. V., E. M. Oleson, K. A. Forney, et al. 2024. "U.S. Pacific Marine Mammal Stock Assessments: 2023."

Chabrerie, A., and F. Arenas. 2024. "What if the Upwelling Weakens? Effects of Rising Temperature and Nutrient Depletion on Coastal Assemblages." *Oecologia* 205: 365–381. https://doi.org/10.1007/s00442-024-05571-6.

Couto, A., N. Queiroz, J. T. Ketchum, et al. 2018. "Smooth Hammerhead Sharks (*Sphyrna zygaena*) Observed off the Portuguese Southern Coast." *Environmental Biology of Fishes* 101, no. 8: 1261–1268. https://doi.org/10.1007/s10641-018-0773-8.

Couto, A., N. Queiroz, P. Relvas, et al. 2017. "Occurrence of Basking Shark *Cetorhinus maximus* in Southern Portuguese Waters: A Two-Decade Survey." *Marine Ecology Progress Series* 564: 77–86. https://doi.org/10.3354/meps12007.

DGRM. 2018. https://www.dgrm.pt/en/am-ec-zonas-maritimas-sob-jurisdicao-ou-soberania-nacional.

Fernandez, M., F. Alves, R. Ferreira, et al. 2021. "Modeling Fine-Scale Cetaceans' Distributions in Oceanic Islands: Madeira Archipelago as a Case Study." *Frontiers in Marine Science* 8: 688248. https://doi.org/10.3389/fmars.2021.688248.

Franks, D. W., G. D. Ruxton, and T. Sherratt. 2025. "Ecology Needs a Causal Overhaul." *Biological Reviews* 100, no. 5: 1950–1969. https://doi.org/10.1111/brv.70029.

Garnier, S., N. Ross, and B. Rudis. 2024. "Colorblind-Friendly Color Maps for R."

Garrido, S., R. Ben-Hamadou, P. B. Oliveira, M. E. Cunha, M. A. Chícharo, and C. D. Van Der Lingen. 2008. "Diet and Feeding Intensity of Sardine Sardina Pilchardus: Correlation With Satellite-Derived Chlorophyll Data." *Marine Ecology Progress Series* 354: 245–256. https://doi.org/10.3354/meps07201.

GEBCO. 2025. "GEBCO." https://download.gebco.net/.

Genner, M. J., J. J. Freer, and L. A. Rutterford. 2017. "Future of the Sea: Biological Responses to Ocean Warming Foresight-Future of the Sea Evidence Review Foresight."

Gilles, A., M. Authier, N. Ramirez-Martinez, et al. 2023. "Estimates of Cetacean Abundance in European Atlantic Waters in Summer 2022 From the SCANS-IV Aerial and Shipboard Surveys." https://tinyurl.com/3ynt6swa.

Hammond, P. S., T. B. Francis, D. Heinemann, et al. 2021. "Estimating the Abundance of Marine Mammal Populations." *Frontiers in Marine Science* 8: 735770. https://doi.org/10.3389/fmars.2021.735770.

Hammond, P. S., C. Lacey, A. Gilles, et al. 2021. "Estimates of Cetacean Abundance in European Atlantic Waters in Summer 2016 From the SCANS-III Aerial and Shipboard Surveys." Sea Mammal Research Unit, University of St Andrews, UK, June, 1–42.

Hartman, K. L., M. Fernandez, and J. M. N. Azevedo. 2014. "Spatial Segregation of Calving and Nursing Risso's Dolphins (Grampus griseus) in the Azores, and Its Conservation Implications." *Marine Biology* 161, no. 6: 1419–1428. https://doi.org/10.1007/s00227-014-2430-x.

Hijmans, R. J. 2023. "Raster: Geographic Data Analysis and Modeling." https://CRAN.R-project.org/package=raster.

Hijmans, R. J. 2025. "Terra: Spatial Data Analysis." https://CRAN.R-project.org/package=terra.

Kaschner, K., N. J. Quick, R. Jewell, R. Williams, and C. M. Harris. 2012. "Global Coverage of Cetacean Line-Transect Surveys: Status Quo, Data Gaps and Future Challenges." *PLoS One* 7, no. 9: e44075. https://doi.org/10.1371/journal.pone.0044075.

Lima, A. R. A., M. Baltazar-Soares, S. Garrido, et al. 2022. "Forecasting Shifts in Habitat Suitability Across the Distribution Range of a Temperate Small Pelagic Fish Under Different Scenarios of Climate Change." *Science of the Total Environment* 804: 150167. https://doi.org/10.1016/j.scitotenv.2021.150167.

MacLeod, C. D. 2009. "Global Climate Change, Range Changes and Potential Implications for the Conservation of Marine Cetaceans: A Review and Synthesis." *Endangered Species Research* 7: 125–136. https://doi.org/10.3354/esr00197.

Marçalo, A., L. Nicolau, J. Giménez, et al. 2018. "Feeding Ecology of the Common Dolphin (Delphinus delphis) in Western Iberian Waters: Has the Decline in Sardine (Sardina pilchardus) Affected Dolphin Diet?" *Marine Biology* 165, no. 3: 44. https://doi.org/10.1007/s00227-018-3285-3.

Marques, T. A., L. Thomas, S. G. Fancy, and S. T. Buckland. 2007. "Improving Estimates of Bird Density Using Multiple-Covariate Distance Sampling." *Auk* 124, no. 4: 1229–1243. https://doi.org/10.1093/auk/124.4.1229.

Martins, M. P., F. L. Matos, A. Cid, et al. 2025. "Habitat Preference of Risso's Dolphins (Grampus griseus) Off the South Coast of Portugal." *Marine Mammal Science* 41, no. 3: 70001. https://doi.org/10.1111/mms.70001.

Mathias, M. d. L., A. Mira, J. Tapisso, et al. 2024. "New Additions to the Mammal List Documented in the Portuguese Red Data Book." *Animals* 14, no. 17: 2514. https://doi.org/10.3390/ani14172514.

Miller, D. L., M. L. Burt, E. A. Rexstad, and L. Thomas. 2013. "Spatial Models for Distance Sampling Data: Recent Developments and Future Directions." *Methods in Ecology and Evolution* 4, no. 11: 1001–1010. https://doi.org/10.1111/2041-210X.12105.

Miller, D. L., E. Rexstad, L. Thomas, J. L. Laake, and L. Marshall. 2019. "Distance Sampling in R." *Journal of Statistical Software* 89, no. 1: 1–28. https://doi.org/10.18637/jss.v089.i01.

Morais, P., L. Afonso, and E. Dias. 2021. "Harnessing the Power of Social Media to Obtain Biodiversity Data About Cetaceans in a Poorly Monitored Area." *Frontiers in Marine Science* 8: 765228. https://doi.org/10.3389/fmars.2021.765228.

Moura, A., C. Silva, SPEA, et al. 2017. *Mamíferos Marinhos-Atlas de Mamíferos de Portugal*. Universidade de Évora.

Moura, A. E., N. Sillero, and A. Rodrigues. 2012. "Common Dolphin (Delphinus delphis) Habitat Preferences Using Data From Two Platforms of Opportunity." *Acta Oecologica* 38: 24–32. https://doi.org/10.1016/j.actao.2011.08.006.

Murphy, S., A. Collet, and E. Rogan. 2005. "Mating Strategy in the Male Common Dolphin (*Delphinus delphis*): What Gonadal Analysis Tells Us." *Journal of Mammalogy* 86, no. 6: 1247–1258. https://doi.org/10.1644/1545-1542(2005)86[1247:MSITMC]2.0.CO;2.

Pante, E., B. Simon-Bouhet, and J.-O. Irisson. 2023. "Marmap: Import, Plot and Analyze Bathymetric and Topographic Data." https://CRAN.R-project.org/package=marmap.

Pike, D. G., T. Gunnlaugsson, B. Mikkelsen, S. D. Halldórsson, and G. A. Víkingsson. 2019. "Estimates of the Abundance of Cetaceans in the Central North Atlantic Based on the NASS Icelandic and Shipboard Surveys Conducted in 2015." *NAMMCO Scientific Publications* 11. https://doi.org/10.7557/3.4941.

QGIS Development Team. 2024. *Qgis Geographic Information System*. QGIS Association.

R Core Team. 2024. *R: A Language and Environment for Statistical Computing*. Foundation for Statistical Computing.

Roberts, J. J., B. D. Best, L. Mannocci, et al. 2016. "Habitat-Based Cetacean Density Models for the U.S. Atlantic and Gulf of Mexico." *Scientific Reports* 6, 22615. https://doi.org/10.1038/srep22615.

Rueda, L., E. Massutí, D. Alvarez-Berastegui, and M. Hidalgo. 2015. "Effect of Intra-Specific Competition, Surface Chlorophyll and Fishing on Spatial Variation of Gadoid's Body Condition." *Ecosphere* 6, no. 10: 1–17. https://doi.org/10.1890/ES15-00087.1.

Sabino-Marques, H. 2005. "Arrojamentos De Cetáceos Na Costa Continental Portuguesa."

Sánchez-Jiménez, A., M. Fujitani, D. MacMillan, A. Schlüter, and M. Wolff. 2019. "Connecting a Trophic Model and Local Ecological Knowledge to Improve Fisheries Management: The Case of Gulf of Nicoya, Costa Rica." *Frontiers in Marine Science* 6: 126. https://doi.org/10.3389/fmars.2019.00126.

Santos, M. B., I. German, D. Correia, et al. 2013. "Long-Term Variation in Common Dolphin Diet in Relation to Prey Abundance." *Marine Ecology Progress Series* 481: 249–268. https://doi.org/10.3354/meps10233.

Sillero, N., S. Arenas-Castro, U. Enriquez-Urzelai, et al. 2021. "Want to Model a Species Niche? A Step-By-Step Guideline on Correlative Ecological Niche Modelling." *Ecological Modelling* 456: 109671. https://doi.org/10.1016/j.ecolmodel.2021.109671.

Silva, A., P. Carrera, J. Massé, et al. 2008. "Geographic Variability of Sardine Growth Across the Northeastern Atlantic and the Mediterranean Sea." *Fisheries Research* 90, no. 1–3: 56–69. https://doi.org/10.1016/j.fishres.2007.09.011.

Sousa, A., M. Fernandez, F. Alves, et al. 2023. "A Novel Expert-Driven Methodology to Develop Thermal Response Curves and Project Habitat Thermal Suitability for Cetaceans Under a Changing Climate." *Science of the Total Environment* 860: 160376. https://doi.org/10.1016/j.scitotenv.2022.160376.

Sousa, M., M. Decastro, I. Alvarez, M. Gesteira, and J. Dias. 2017. "Why Coastal Upwelling Is Expected to Increase Along the Western Iberian Peninsula Over the Next Century?" *Science of the Total Environment* 592: 243–251. https://doi.org/10.1016/j.scitotenv.2017.03.046.

Sousa, M., A. Ribeiro, M. Des, M. Gesteira, M. Decastro, and J. Dias. 2020. "NW Iberian Peninsula Coastal Upwelling Future Weakening: Competition Between Wind Intensification and Surface Heating." *Science of the Total Environment* 703: 134808. https://doi.org/10.1016/j.scitotenv.2019.134808.

Tasker, M. L., P. H. Jones, T. Dixon, and B. F. Blake. 1984. "Counting Seabirds at Sea From Ships: A Review of Methods Employed and a Suggestion for a Standardized Approach." *Auk* 101, no. 3: 567–577. https://doi.org/10.1093/auk/101.3.567.

Vingada, J. V., and C. Eira. 2018. "Conservação de Cetáceos e Aves Marinhas em Portugal Continental. O projeto LIFE+ MarPro." In *LIFE+ MarPro*, 258. Universidade de Aveiro.

Virgili, A., H. Araújo, A. Astarloa Diaz, et al. 2024. "Seasonal Distribution of Cetaceans in the European Atlantic and Mediterranean Waters." *Frontiers in Marine Science* 11: 1319791. https://doi.org/10.3389/fmars.2024.1319791.

Weir, J. S., N. M. T. Duprey, and B. Würsig. 2008. "Dusky Dolphin (*Lagenorhynchus obscurus*) Subgroup Distribution: Are Shallow Waters a Refuge for Nursery Groups?" *Canadian Journal of Zoology* 86, no. 11: 1225–1234. https://doi.org/10.1139/Z08-101.

Wickham, H., W. Chang, L. Henry, et al. 2024. "Create Elegant Data Visualisations Using the Grammar of Graphics."

Würsig, B., S. Lynn, T. Jefferson, and K. Mullin. 1998. "Behavior of Cetaceans in the Northern Gulf of Mexico Relative to Survey Ships and Aircraft." *Aquatic Mammals* 24, no. 1: 41–50.

Zwolinski, J., P. Oliveira, V. Quintino, and Y. Stratoudakis. 2010. "Sardine Potential Habitat and Environmental Forcing off Western Portugal." *ICES Journal of Marine Science* 67, no. 8: 1553–1564. https://doi.org/10.1093/icesjms/fsq068.

Supporting Information

Additional supporting information can be found online in the Supporting Information section. **Data S1:** Supporting Information. **Data S2:** Supporting Information. **Table S1:** Summary of generalized additive models considered in this study. [*] indicates the selected model. **Table S2:** Summary of detection functions tested for modeling common dolphin detectability according to the distance to the observer. [*] indicates the selected function. Since there were few records with sea state ≥ 4, all of these were aggregated in a single level for the factor sea state covariate. **Table S3:** Comparison between SCANS-III (Hammond, Lacey, et al. 2021) and SCANS-IV (Gilles et al. 2023) surveys and final model predictions in their respective blocks. NA stands for not applicable. * Since SCANS-III blocks overlap with the Spanish coast, instead of absolute abundance, average density confidence intervals for SCANS-III blocks are compared with their overlapping area with this study's study area. ** Model-based abundance estimates for SCANS-IV blocks were done for summer 2020, the year in our dataset closest to the SCANS-IV survey. **Figure S1:** Correlation matrix of variables considered for modeling common dolphin density. **Figure S2:** Smoothed fits of predictors, showing how the estimated common dolphin density varies according the environmental gradient. **Figure S3:** Diagnostic plots of the selected model. **Figure S4:** Plots of tested detection functions. From top to bottom, left to right: half-normal key with 0 cosine adjustments, with continuous sea state, with sea state as a factor variable, respectively; uniform key with 0, 1 and 2 cosine adjustments, respectively; hazard-rate key with 0 cosine adjustments, with continuous sea state, with sea state as a factor variable, respectively. **Figure S5:** Predicted common dolphin density distribution in mainland Portugal coastal waters in 2004, according to the season. **Figure S6:** Predicted common dolphin density distribution in mainland Portugal coastal waters in 2005, according to the season. **Figure S7:** Predicted common dolphin density distribution in mainland Portugal coastal waters in 2006, according to the season. **Figure S8:** Predicted common dolphin density distribution in mainland Portugal coastal waters in 2007, according to the season. **Figure S9:** Predicted common dolphin density distribution in mainland Portugal coastal waters in 2008, according to the season. **Figure S10:** Predicted common dolphin density distribution in mainland Portugal coastal waters in 2009, according to the season. **Figure S11:** Predicted common dolphin density distribution in mainland Portugal coastal waters in 2010, according to the season. **Figure S12:** Predicted common dolphin density distribution in mainland Portugal coastal waters in 2011, according to the season. **Figure S13:** Predicted common dolphin density distribution in mainland Portugal coastal waters in 2012, according to the season. **Figure S14:** Predicted common dolphin density distribution in mainland Portugal coastal waters in 2013, according to the season. **Figure S15:** Predicted common dolphin density distribution in mainland Portugal coastal waters in 2014, according to the season. **Figure S16:** Predicted common dolphin density distribution in mainland Portugal coastal waters in 2015, according to the season. **Figure S17:** Predicted common dolphin density distribution in mainland Portugal coastal waters in 2016, according to the season. **Figure S18:** Predicted common dolphin density distribution in mainland Portugal coastal waters in 2017, according to the season. **Figure S19:** Predicted common dolphin density distribution in mainland Portugal coastal waters in 2018, according to the season. **Figure S20:** Predicted common dolphin density distribution in mainland Portugal coastal waters in 2019, according to the season. **Figure S21:** Predicted common dolphin density distribution in mainland Portugal EEZ in 2004, according to the season. **Figure S22:** Predicted common dolphin density distribution in mainland Portugal EEZ in 2005, according to the season. **Figure S23:** Predicted common dolphin density distribution in mainland Portugal EEZ in 2006, according to the season. **Figure S24:** Predicted common dolphin density distribution in mainland Portugal EEZ in 2007, according to the season. **Figure S25:** Predicted common dolphin density distribution in mainland Portugal EEZ in 2008, according to the season. **Figure S26:** Predicted common dolphin density distribution in mainland Portugal EEZ in 2009, according to the season. **Figure S27:** Predicted common dolphin density distribution in mainland Portugal EEZ in 2010, according to the season. **Figure S28:** Predicted common dolphin density distribution in mainland Portugal EEZ in 2011, according to the season. **Figure S29:** Predicted common dolphin density distribution in mainland Portugal EEZ in 2012, according to the season. **Figure S30:** Predicted common dolphin density distribution in mainland Portugal EEZ in 2013, according to the season. **Figure S31:** Predicted common dolphin density distribution in mainland Portugal EEZ in 2014, according to the season. **Figure S32:** Predicted common dolphin density distribution in mainland Portugal EEZ in 2015, according to the season. **Figure S33:** Predicted common dolphin density distribution in mainland Portugal EEZ in 2016, according to the season. **Figure S34:** Predicted common dolphin density distribution in mainland Portugal EEZ in 2017, according to the season. **Figure S35:** Predicted common dolphin density distribution in mainland Portugal EEZ in 2018, according to the season. **Figure S36:** Predicted common dolphin density distribution in mainland Portugal EEZ in 2019, according to the season.